

Heaven's Light is Our Guide



DEPARTMENT OF COMPUTER SCIENCE & ENGINEERING

Rajshahi University of Engineering & Technology, Bangladesh

**Surface Crack Detection Using Deep Convolutional Neural
Network**

Author

Sadman Sakib Radh

Roll No. 1503007

Department of Computer Science & Engineering
Rajshahi University of Engineering & Technology

Supervised by

Prof . Dr. Md. Al Mamun

Professor

Department of Computer Science & Engineering
Rajshahi University of Engineering & Technology

ACKNOWLEDGEMENT

At first, I would like to thank the Almighty Allah for giving us the opportunity and enthusiasm along the way for the completion of our thesis work.

We would like to express our sincere appreciation, gratitude, and respect to our supervisor Prof. Dr. Al Mamun, Professor of Department of Computer Science and Engineering, Rajshahi University of Engineering and Technology, Rajshahi. Throughout the year he has not only given us technical guidelines, advice and necessary documents to complete the work he has also given us continuous encouragement, advice, help and sympathetic co-operation whenever he deemed necessary. His continuous support was the most successful tool that helped us to achieve our result. Whenever we were stuck in any complex problems or situation he was there for us at any time of the day. Without his sincere care, this work has not been materialized in the final form that it is now at the present.

I am also grateful to all the respective teachers of Computer Science and Engineering, Rajshahi University of Engineering and Technology, Rajshahi for good & valuable suggestions and inspirations from time to time.

Finally, I convey my thanks to my parents, friends, and well-wishers for their constant inspirations and many helpful aids throughout this work.

December 6, 2020
RUET,Rajshahi

Sadman Sakib Radh

Heaven's Light is Our Guide



DEPARTMENT OF COMPUTER SCIENCE & ENGINEERING

Rajshahi University of Engineering & Technology, Bangladesh

CERTIFICATE

*This is to certify that this thesis report entitled “**Surface Crack Detection using Deep Convolutional Neural Network**” submitted by **Sadman Sakib Radh, Roll: 1503007** in partial fulfillment of the requirement for the award of the degree of Bachelor of Science in Computer Science & Engineering of Rajshahi University of Engineering & Technology, Bangladesh is a record of the candidate own work carried out by him under my supervision. This thesis has not been submitted for the award of any other degree*

Supervisor

External Examine

Prof. Dr. Md. Al Mamun

Professor

Department of Computer Science & Engineering

Rajshahi University of Engineering & Technology

Rajshahi-6204

ABSTRACT

Crack detection has a major importance for justifying structural health of buildings and roads. As Bangladesh is a densely populated country with a large number of traffic, it is very important to monitor the roads correctly and reduce the chance of accidents and other uncertainty both in roads and buildings. But the task is challenging for computer vision method as cracks have only low-level features for detection which are easily confused with background texture and irregularities in construction. Also the manual process of crack detection is unfeasible and time consuming. And the result may not also be accurate all the time. That's why we are proposing a Machine Learning based algorithm, Deep Convolutional Neural Networks(CNN) for detecting cracks of roads as well as buildings as Convolutional Neural Network is a promising method with higher accuracy and precision. Quantitative evaluation conducted on a data set of 4000 images of size 227×227 pixels, are classified in two classes based on the crack and non-crack images. The images are reshaped, rescaled to feed the algorithm while necessary. Throughout the paper we will discuss about the comparative study of CNN for detecting cracks.

Key words: Crack detection, Image processing, Deep Convolutional Neural Network

CONTENTS

	Page No.
ACKNOWLEDGEMENT	i
CERTIFICATE	ii
ABSTRACT	iii
CHAPTER 1	
Introduction	1
1.1 Introduction	1
1.2 Motivation	2
1.3 Literature Review	2
1.4 Thesis Contribution	4
1.5 Thesis Organization	5
CHAPTER 2	
Object Recognition in Computer	6-14
2.1 Computer Vision	6
2.2 Object Recognition	7
2.2.1 An Example	8
2.2.2 Challenges	8
2.2.3 The Image Classification Pipeline	10
2.3 Linear Classifier	11
2.3.1 Score Function	11
2.3.2 Loss Function: Softmax Function	12
2.3.3 One Hot Encoding	13
2.2 Conclusion	14
CHAPTER 3	
Neural Networks (NN)	15-26

3.1 NN	15
3.2 Biological Motivation and Connections	15
3.3 Neural Network Architectures	17
3.4 Data Preprocessing	18
3.5 Weight Initialization	19
3.6 Regularization	19
3.7 Loss Function	21
3.8 Learning	22
3.8.1 Backpropagation	22
3.8.2 Gradient Checks	24
3.8.3 Learning Rate	25
3.8.4 Per-Parameter Adaptive Learning Rate Methods	25
3.9 Conclusion	26
 CHAPTER 4	
Convolutional Neural Networks (CNN)	27-39
4.1 CNN	27
4.2 CNN Architecture	28
4.3 Layers in CNN	29
4.3.1 Convolutional Layer	30
4.3.2 Activation Layer	33
4.3.3 Pooling Layer	35
4.3.4 Fully-Connected (FC) Layer	37
4.4 Known Architectures in CNN	38
4.5 Conclusion	39
 CHAPTER 5	
Methodology	40-45
5.1 Data Source	40
5.1.2 Data Preprocessing	41
5.2 Model Architecture and Training	42
5.4 Conclusion	45

CHAPTER 6

Results and Performance Analysis 46-49

6.1 Environment 46

6.2 Experimental Analysis 46

6.3 Conclusion 49

CHAPTER 7

Conclusion and Future Works 50-51

7.1 Summary 50

7.2 Limitations 50

7.3 Future Work 51

7.4 Conclusion 51

REFERENCES 52-58

LIST OF TABLES

Table Number	Table Title	Page No.
5.1	Model Summary	43
6.1	The proposed system achieved the state of the art result	48

LIST OF FIGURES

Figure Number	Figure Caption	Page No.
2.1	Computer Vision Tasks	7
2.2	Object recognition of different class objects	7
2.3	An example of object recognition	8
2.4	Challenges in object recognition	9
2.5	CIFAR 10 dataset	10
2.6	An example of a linear classifier to failing predict correct class	12
2.7	Linear classifier for high dimensional points	12
2.8	A one hot encoding example	14
3.1	A biological neuron (top) and a common mathematical model (bottom)	16
3.2	An example of a 3-layer neural network	17
3.3	Preprocessing the data	18
3.4	Dropout used in a network	21
3.5	The change to a hidden to output weight depends on error	22
3.6	Loss function is changing with different learning rates	25
4.1	Comparison of an original Neural Network with a CNN	29
4.2	A typical CNN architecture	30

4.3	ConvNet architecture example	30
4.4	Convolution layer example	31
4.5	Example of local connectivity	32
4.6	Activation function: tanh	35
4.7	Activation function: ReLU	35
4.8	Example of maxpooling	36
5.1	No of Crack and Non Crack images	40
5.2	Non Crack and Crack Images	41
5.3	Example of reshaped crack image	42
5.4	The architecture of implemented CNN	43
6.1	Example of annotated concrete crack images	47
6.2	Accuracy Curve for training and validation	47

CHAPTER 1

Introduction

1.1 Introduction

Crack detection refers to the process of detecting defects in impermeable materials or surfaces like metals, concrete, ceramics etc. It is very crucial in the inspection and maintenance of concrete as well as roads structures. Traditional approach for crack detection is visual inspection by a trained inspector who evaluates the condition of any surface according to the location and width of a crack. This manual process is very time consuming and is also unfeasible since a building or road may have many cracks at a certain time. And the detection result may not also be accurate all the time.

Given the human weakness of inspection, image-based crack detection method is deeply studied. Image processing techniques identify cracks from images based on some assumptions that the cracks are slender and connected regions and darker than their backgrounds [1]. About morphology, it usually segments cracks using just right threshold [2]. For further robustness of crack detection, general global transforms and local edge detections are deployed [3-5], such as fast Haar transform, fast Fourier transform, Sobel and Canny edge detectors, etc. Fortunately, this approach excessively depends on well-chosen image preprocessing techniques and image edge detection. And the features on structure surface are variable and affected by many factors in real situation, such as light, shadows etc.

To detect cracks from images more accurately, machine learning-based approaches are utilized [6]. Artificial neural networks, supervised machine learning algorithms, are used to classify images that are with or without cracks [7]. However, because of the limitation of computational capability, only simple structures of artificial neural networks can be used to detect cracks in practice. In recent years, thanks to the development of deep learning and parallel computations using graphic processing units (GPUs) [8], deep CNNs have been highlighted in image recognition [9].

Unlike conventional neural networks, CNNs classifying images depend on fewer computations due to the partial connections, sharing weights and pooling process between neurons. Notably, designing CNN architecture is needed, and a databank that contains large number of images should be built to train the CNN [10]. With the popularity of smartphones, smartphones has been used as tools for structure health monitoring [11].

In this paper, a deep CNN network is applied as a classifier for detecting surface crack. The CNN based crack detection can verify cracks from images and the detection result will not be affected by noise on surface or road images.

1.2 Motivation

Technological development is going on day by day. The old one is being replaced by the new one. Machine learning based technology is now getting higher popularity. Effective use of such technology is seen in many areas like medical, face recognition etc. As it is a vital issue for safe driving in highways, it is important to ensure the roads are safe. So we need more accuracy with less computational time. And this is only possible through machine based approach like CNN or other models. Some works have been done in this sector and those works have motivated us to develop a classification system that can classify surface crack.

1.3 Literature Review

The section is about reviewing some existing works that are related to crack detection. There have been various studies on the road-traffic conditions, causes and their effects in the socio-economic, physical and mental health the people of Bangladesh [12][13][14]. For pattern recognition, image processing, object identification, semantic and instance segmentation, CNN based machine learning models are very efficiently used. So far, the “AlexNet” architecture introduced by Krizhevsky Et al. [15] has been successfully applied in a number of computer vision tasks, for example in object detection [6], object tracking [16], segmentation, [17] video classification, [18] human pose estimation [19] and super resolution [20].

Classical deep Neural Networks like CNN and FCN extract image features finding key points and thus are used for 2D image classification. On the other hand, Google introduced their own residual deep neural network architecture in Inception-v1, they have optimized the network furthermore through Inception-v3 to reduce computational cost [19][20]. The basic difference between Inception-v3 and Inception-v4 is that the latter one has a simpler architecture and more inception modules [21]. The constraints contained in Inception-v3 had come from the need for partitioning model architecture with distributed training using DistBelief [22]. With migration to TensorFlow [23] those constraints have been lifted which allowed the reintroduced architecture to get simplified.

The goal of this research is to classify crack of any surface or road by using deep convolutional neural network and maximizing the accuracy. 40,000 of crack and non crack images are used for this network. Among them 20,000 are positive (crack) and rest 20,000 are negative (non crack). CNN has been used successfully in 2D image recognition and research centered on image processing such as: Food Classification [24] and Gaussian noise detection [25]. For this reason, CNN is used to classify crack images. In this analysis, the qualified model evaluated the pixel strength adjustment for the presence of holes, dumps, surface water and change in road color for hilly tracts and change in soil.

CNN based researches have been performed to detect road, semantic segmentation of road scenes [26-30], road-lane, road area extraction [31], rural roads detection [32], street signs detection and so on. The works are most commonly based on classification, object detection or semantic segmentation. For image recognition and object-detection based works some of the novel approaches have been introduced by Lin et al. [33], Simonyan et al. in VGGNet [34] and GoogleNet (Inception - v1) [35] by Szegedy Et al. Residual connections were introduced in [14]. In civil engineering ventures, deep convolutionary neural network approaches such as bounding box approaches in computer vision-based models have been suggested for surface health monitoring. A model of pothole identification was also proposed[36] based on semantic segmentation on concrete crack images, which is also a fully connected network (FCN) solution. Several semantic image segmentation models have been introduced there by [37-41].

1.4 Thesis Contribution

- i. An automated system is created using Convolutional Neural Network (CNN).
- ii. The system has the ability to distinguish between crack and non-crack images if it is trained with a large enough dataset.
- iii. In the training process, it learns the features of different types of crack and then classifies with the learned knowledge.
- iv. This model can be used in civil engineering sectors.
- v. The model leaves opportunities for further improvement and it can be modified for even better results in the future.

1.5 Thesis Organization

The rest of the thesis is organized as follows:

Chapter 2 - Object Recognition in Computer Vision

This section describes what computer vision and object recognition are and what the challenges and overall computer vision pipeline are. It also describes linear classifier.

Chapter 3 - Neural Networks

This chapter discusses the architecture, data preprocessing, weights initialization, loss function, regularization and how learning is achieved in neural networks.

Chapter 4 - Convolutional Neural Network

This chapter discusses the architecture, layers and some known popular convolutional neural network models available right now. It also distinguishes the differences between an ordinary neural network and a convolutional neural network.

Chapter 5 - Implementation

This chapter describes about the datasets, data preprocessing, the whole work flow of the developed architecture.

Chapter 6 - Result Analysis

This chapter describes the datasets that are used and the overall result of the developed architecture. It also shows the performance of the architecture.

Chapter 7 - Conclusion and Future Work

This chapter concludes the thesis, describes its limitation and shows a direction of future work.

1.6 Conclusion

Detecting crack is a vital issue in civil engineering. As we are a densely populated country with a large number of vehicles we need to keep the roads safe. The thesis introduces an automated system which can solve this problem.

CHAPTER 2

Object Recognition in Computer Vision

This chapter starts by describing briefly what computer vision is and then later gives an introduction, method and challenges of object recognition. In the latter part of the chapter, the linear classifier for recognizing objects have been discussed. As the research is based on recognizing crack in surfaces this part is pretty significant to the research work.

2.1 Computer Vision

Computer vision is an interdisciplinary field that deals with how computers can be made for gaining high-level understanding from digital images or videos. High level understanding includes recognizing what the object is (e.g. dog, cat, car etc.), semantic segmentation, classifying using localization to detect a single object in a given scene, instant segmentation and many other tasks depicted in figure 2.1. Computer vision is concerned with the theory behind artificial systems that extract information from images. It seeks to automate tasks that an animal visual system can do. The target behind computer vision is to create such a system that would be as efficient in recognizing objects and do further actions depending on what kind of object as the human brain sees and does. Almost 50% neurons of a human's cortex are involved in visual processing [42]. Computer vision aims to mimic the working principles of visual processing in computer processors.

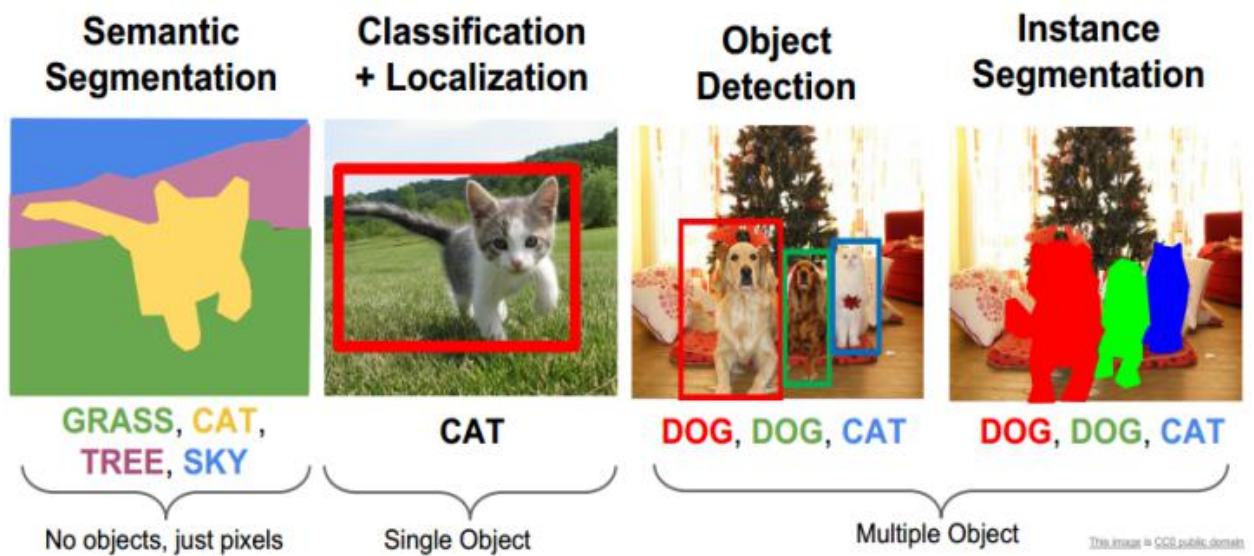


Figure 2.1: Computer Vision Tasks [42]

2.1 Object Recognition

Object recognition is the task of assigning an input image one label from a fixed set of categories. It creates a model that most accurately classifies objects in the given images of the dataset. This is one of the core problems in Computer Vision that, despite its simplicity, has a large variety of practical applications. Figure 2.2 depicts the recognition of different objects.



Figure 2.2: Object recognition of different class objects [42]

2.2.1 An Example

In the image of figure 2.3 an object recognition model takes a single image and assigns probabilities to 4 labels, {cat, dog, hat, mug}. As shown in the image, an image is represented as one large 3-dimensional array of numbers. In this example, the cat image is 248 pixels wide, 400 pixels tall, and has three color channels Red, Green, Blue (or RGB). Therefore, the image consists of $248 \times 400 \times 3$ numbers or a total of 297,600 numbers. Each number is an integer that ranges from 0 (black) to 255 (white). The task will be to turn this quarter of a million numbers into a single label, such as “cat”.

The task in object recognition is to predict a single label (or a distribution over labels as shown here to indicate our confidence) for a given image. Images are 3-dimensional arrays of integers from 0 to 255, of size Width x Height x 3. The 3 represents the three-color channels Red, Green, Blue.

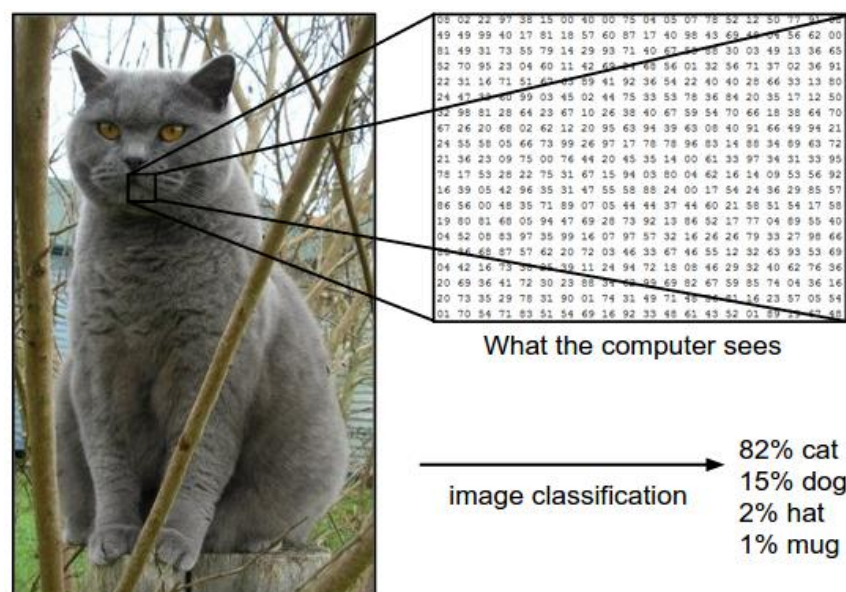


Figure 2.3: An example of object recognition [42]

2.2.2 Challenges

Since this task of recognizing a visual concept (e.g. cat) is relatively trivial for a human to perform, it is worth considering the challenges involved from the

perspective of a Computer Vision algorithm. A list of challenges for the computer in the raw representation of images as a 3-D array of brightness values:

- **Viewpoint variation.** A single instance of an object can be oriented in many ways with respect to the camera.
- **Scale variation.** Visual classes often exhibit variation in their size (size in the real world, not only in terms of their extent in the image).
- **Deformation.** Many objects of interest are not rigid bodies and can be deformed in extreme ways.
- **Occlusion.** The objects of interest can be occluded. Sometimes only a small portion of an object (as little as few pixels) could be visible.
- **Illumination conditions.** The effects of illumination are drastic on the pixel level.
- **Background clutter.** The objects of interest may blend into their environment, making them hard to identify.
- **Intra-class variation.** The classes of interest can often be relatively broad, such as chair. There are many different types of these objects, each with their own appearance.

A good image classification model must be invariant to the cross product of all these variations, while simultaneously retaining sensitivity to the inter-class variations. Figure 2.4 shows the different challenges for a specific class.

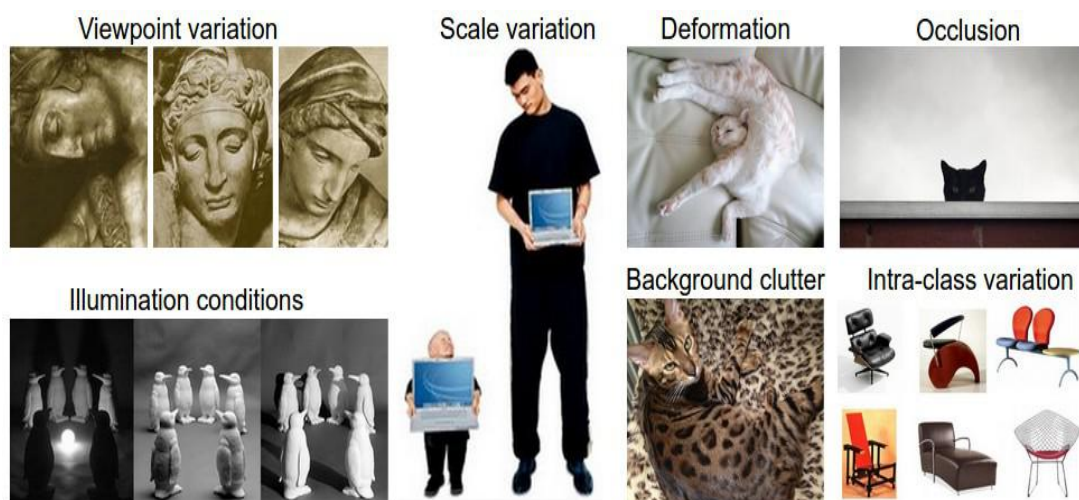


Figure 2.4: Challenges in object recognition [42]

The challenge is to write an algorithm that can classify images into distinct categories. Instead of trying to specify what every one of the categories of interest looks like directly in code, the method is to provide the computer with many examples of each class and then develop learning algorithms that look at these examples and learn about the visual appearance of each class. This approach is referred to as a data-driven approach since it relies on first accumulating a training dataset of labeled images. An example of this kind would be the CIFAR10 dataset which consists of 10 classes of 50,000 training images and 10,000 testing images shown in figure 2.5.

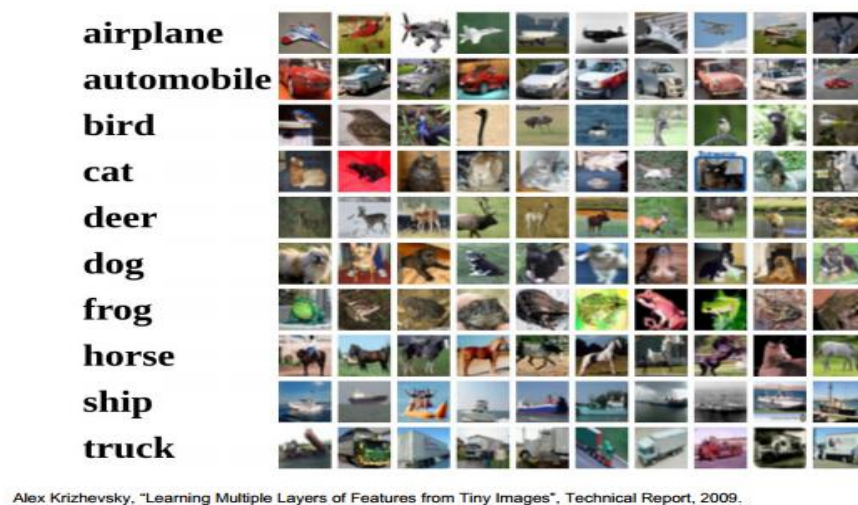


Figure 2.5: CIFAR 10 dataset

2.2.3 The Image Classification Pipeline

The task in object recognition is to take an array of pixels that represents a single image and assign a label to it. The complete pipeline can be formalized as follows:

- **Input:** The input consists of a set of N images, each labeled with one of K different classes. This data is referred to as the training set.
- **Learning:** The learning uses the training set to learn what every one of the classes looks like. This step is referred to as training a classifier or learning a model.
- **Evaluation:** At the last step, the quality of the classifier is evaluated by asking it to predict labels for a new set of images that it has never seen before. Then it will be compared with the true labels of these images to the ones predicted by the classifier.

2.3 Linear Classifier

An approach to object recognition that we will eventually naturally extend to entire Neural Networks and Convolutional Neural Networks. The approach will have two major components: a score function that maps the raw data to class scores, and a loss function that quantifies the agreement between the predicted scores and the ground truth labels.

2.3.1 Score Function

A training dataset of images $y_i \in R^D$, each associated with a label y_i . Here $i = 1 \dots N$ and $y_i \in 1 \dots N$. Total of N examples (each with a dimension of D) and K distinct categories. Then a linear mapping can be defined as:

$$f(x_i, W, b) = Wx_i + b \quad (1)$$

In the above equation, the image x_i has all of its pixels flattened out to a single column vector of shape $[D \times 1]$. The matrix W (of size $[K \times D]$), and the vector b (of size $[K \times 1]$) are the parameters of the function. The parameters in W are weights, and b is called the bias vector because it influences the output scores, but without interacting with the actual data x_i . The weights are essential in order to classify the object. In Figure 2.6 explains a linear classifier for an image only having 4 pixels and having only 3 classes (red (cat), green (dog), blue (ship) class). In this classifier, dog score has the highest, meaning it is classifying a cat as dog because of the weights which need to be changed to get the actual results. The next section, it is shown how a loss function changes these weights to get a better result.

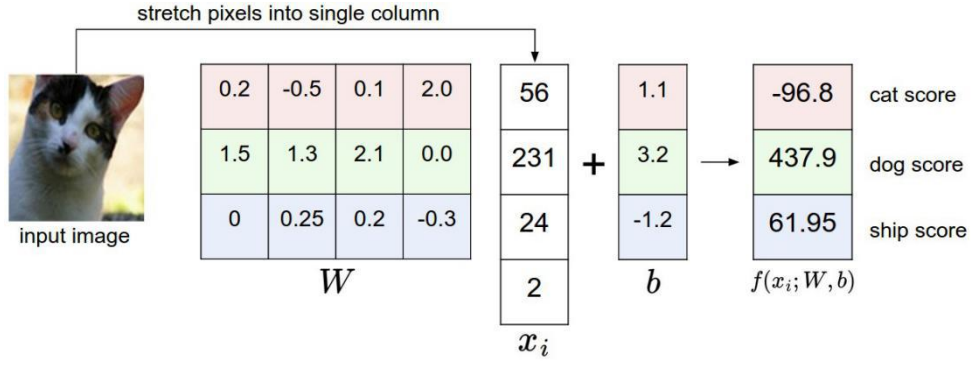


Figure 2.6: An example of a linear classifier to failing to predict correct class [42]

And figure 2.7 depicts the analogy of images as high-dimensional points.

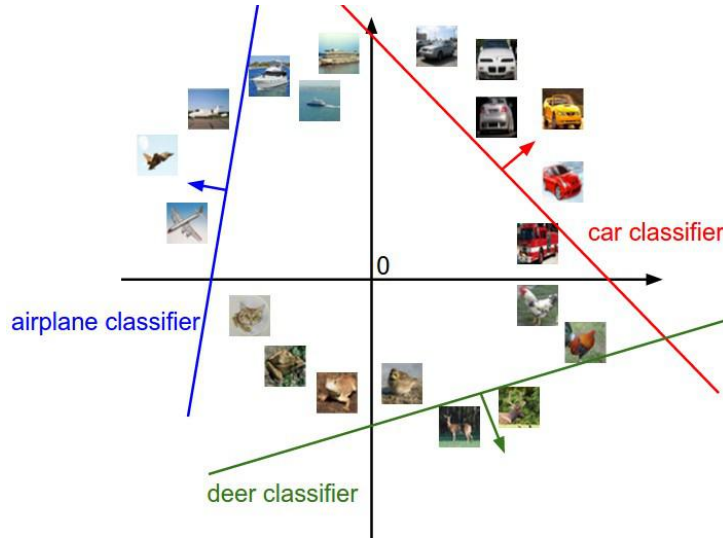


Figure 2.7: Linear classifier for high dimensional points [42]

2.3.2 Loss Function: Softmax Function

In the previous section, a function from the pixel values to class scores, which was parameterized by a set of weights W . As the data cannot be changed, the weights are changed to minimize the loss of the predicted class with the actual class. As seen in the previous section how the classifier failed to predict the correct class. The loss function will determine this outcome to predict the amount of loss in a particular prediction. The loss function softmax is discussed here as it is used the research.

The Softmax classifier computes “probabilities” for all labels. For example, given an image, the softmax classifier compute the probabilities of the three labels as $[0.9, 0.09, 0.01]$ for the classes “cat”, “dog” and “ship” which interpret its confidence in

each class. In the softmax classifier, we interpret the scores as the non normalized log probabilities for each class and calculate loss with a cross-entropy loss that has the form:

$$L_i = -\log\left(\frac{e^{f_{y_i}}}{\sum_j e^{f_j}}\right) \quad (2)$$

The notation f_j means the j th element of the vector of class scores f . The full loss for the dataset is the mean of L_i over all training examples together. The function $f_j(z) = \frac{e^{z_j}}{\sum_k e^{z_k}}$ is called the softmax function: It takes a vector of arbitrary real-valued scores (in z) and squashes it to a vector of values between zero and one that sum to one. The cross-entropy between a “true” distribution p and an “estimated” distribution q is defined as:

$$H(p, q) = -\sum p(x) \log q(x) \quad (3)$$

The Softmax classifier is hence minimizing the cross-entropy between the estimated class probabilities ($q = \frac{e^{f_{y_i}}}{\sum_j e^{f_j}}$ as seen above) and the “true” distribution, which in this interpretation is the distribution where all probability mass is on the correct class (i.e. $p = [0, \dots, 1, \dots, 0]$ contains a single 1 at the y_i position.).

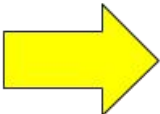
2.3.2 One Hot Encoding

Many machine learning algorithms cannot operate on label data directly. They require all input variables and output variables to be numeric. In general, this is mostly a constraint of the efficient implementation of machine learning algorithms rather than hard limitations on the algorithms themselves. This means that categorical data must be converted into a numerical form. If the categorical variable is an output variable, we may also want to convert predictions by the model back into a categorical form in order to present them or use them in some application.

One hot encoding [43] is a process by which categorical variables are converted into a form that could be provided to machine learning algorithms to achieve better results in prediction. We use one hot encoder to perform “binarization” of the category and include it as a feature to train the model. The first requirement is that the categorical values be mapped to integer values. Then, each integer value is

represented as a binary vector that is all zero values except the index of the integer, which is marked with a 1.

One hot encoding creates new (binary) columns, indicating the presence of each possible value from the original data. An example of one hot encoding is showed in figure 2.8, the values in the original data are Red, Yellow, and Green. We create a separate column for each possible value. Wherever the original value was Red, we put a 1 in the Red column.



Color
Red
Red
Yellow
Green
Yellow

Red	Yellow	Green
1	0	0
1	0	0
0	1	0
0	0	1

Figure 2.8: A one hot encoding example [44]

2.4 Conclusion

Object recognition is a part of a greater field i.e. computer vision which the process of imitating the vision system of humans. A good classifier is needed for the computer to classify objects with the minimum of loss from the actual results. While working with categorical data, we need a way to turn this into a numerical value.

CHAPTER 3

Neural Networks (NN)

This chapter discusses different sections of the neural network. Neural network's motivation and its architecture are briefly explained here. The latter part discusses how the model gets to build and how it is learned through the process.

3.1 NN

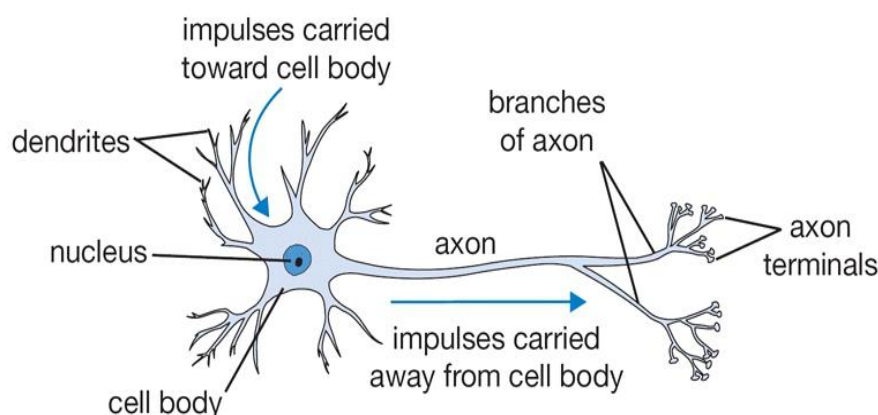
Image classification based on some particular visual information has always been a difficult task even for the human visual system. Considering the microscopic images from histopathological sections, they are much more difficult to classify because of their complex geometrical shape as well as the inter-intraclass variability in the images [44]. Neural network is a trainable deep learning architecture. This was encouraged by animal optical system [45] that learns features directly from the given input data avoiding the hand-crafted feature. It consists of multiple nonlinear transformations in several steps and in each step, it works to reduce the error to accurately classify.

3.2 Biological Motivation and Connections

To develop an artificial intelligence, researchers created a highly interconnected system by using the combination of simple computing elements which mimics the working method of a human brain. At first, researchers were trying to imitate the neurophysiology of the brain [45] and these elements acted as the neurons of a brain. As the modern neural networks now are incorporated with different numerical analysis methods, they can make predictions about different real-world problems [45]. The basic computational unit of the brain is a neuron. Approximately 86 billion neurons can be found in the human nervous system and they are connected with approximately 10^{14} - 10^{15} synapses [45]. Figure 3.1 shows a drawing of a biological neuron (top) and a common mathematical model (bottom).

Each neuron receives input signals from its dendrites and produces output signals along its (single) axon. The axon eventually branches out and connects via synapses to dendrites of other neurons. In the computational model of a neuron, the signals that travel along the axons (e.g. x_0) interact multiplicatively (e.g. w_0x_0) with the dendrites of the other neuron based on the synaptic strength at that synapse (e.g. w_0).

The idea is that the synaptic strengths (the weights w) are learnable and control the strength of influence of one neuron on another. In the basic model, the dendrites carry the signal to the cell body where they all get summed. If the final sum is above a certain threshold, the neuron can fire, sending a spike along its axon. In the computational model, we assume that the precise timings of the spikes do not matter and that only the frequency of the firing communicates information. Based on this rate code interpretation, we model the firing rate of the neuron with an activation function f , which represents the frequency of the spikes along the axon. Historically, a common choice of activation function is the sigmoid function σ , since it takes a real-valued input (the signal strength after the sum) and squashes it to range between 0 and 1. So, each neuron performs a dot product with the input and its weights, adds the bias and applies the non-linearity (or activation function).



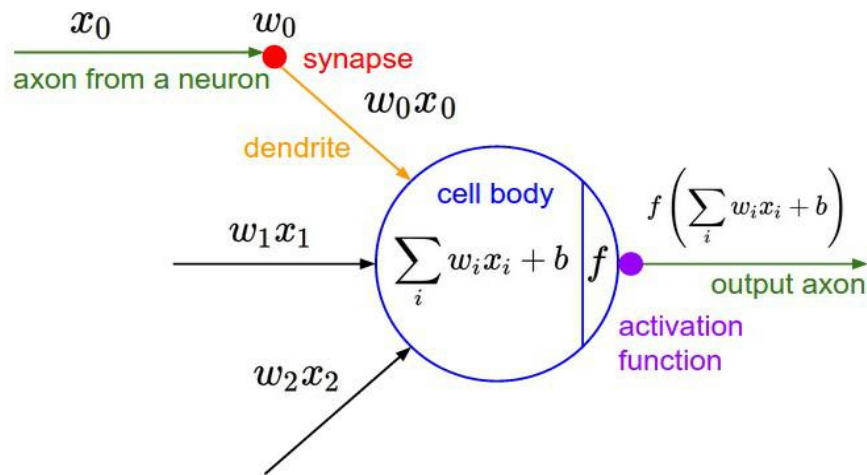


Figure 3.1: A biological neuron (top) and a common mathematical model (bottom)
[42]

3.3 Neural Network Architectures

Neural Networks are modeled as collections of neurons that are connected in an acyclic graph. In other words, the outputs of some neurons can become inputs to other neurons. Cycles are not allowed since that would imply an infinite loop in the forward pass of a network. Instead of an amorphous blob of connected neurons, Neural Network models are often organized into distinct layers of neurons. For regular neural networks, the most common layer type is the fully-connected layer in which neurons between two adjacent layers are fully pairwise connected, but neurons within a single layer share no connections. Figure 3.2 shows a 3-layer neural network with three inputs, two hidden layers of 4 neurons each and one output layer. In both cases there are connections (synapses) between neurons across layers, but not within a layer.

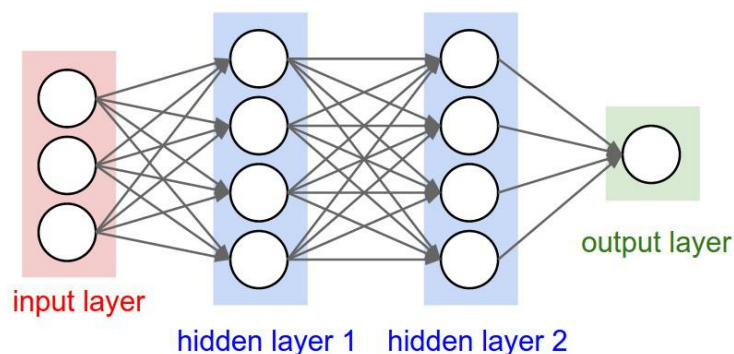


Figure 3.2: An example of a 3-layer neural network [42]

3.4 Data Preprocessing

Some data preprocessing techniques are used in neural network to involves transforming raw data into an understandable format. Mean subtraction is the most common form of preprocessing. It involves subtracting the mean across every individual feature in the data and has the geometric interpretation of centering the cloud of data around the origin along every dimension.

Normalization refers to normalizing the data dimensions so that they are of approximately the same scale. There are two common ways of achieving this normalization. One is to divide each dimension by its standard deviation, once it has been zero-centered. Another form of this preprocessing normalizes each dimension so that the min and max along the dimension is -1 and 1 respectively. It is only used when different input features have different scales (or units), but they should be of approximately equal importance to the learning algorithm.

Common data preprocessing pipeline includes the original data, 2-dimensional input data is firstly zero-centered by subtracting the mean in each dimension. The data cloud then gets centered around the origin. Each dimension is additionally scaled by its standard deviation. Figure 3.3 shows this process in three steps. the red lines in the figure indicate the extent of the data - they are of unequal length in the middle, but of equal length on the right.

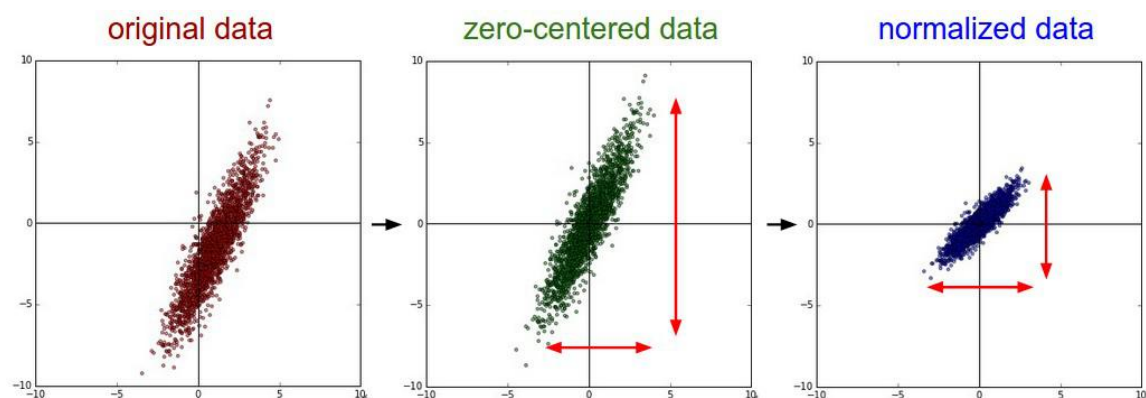


Figure 3.3: Preprocessing the data [42]

3.5 Weight Initialization

Before training the network, the convention is to initialize its parameters. A reasonable-sounding idea might be to set all the initial weights to zero, which is the expectation of “best guess” in expectation. But if every neuron in the network computes the same output, then they will also all compute the same gradients during backpropagation and undergo the exact same parameter updates. In other words, there is no source of asymmetry between neurons if their weights are initialized to be the same. As a solution, it is common to initialize the weights of the neurons to small numbers and refer to doing so as symmetry breaking. The idea is that the neurons are all random and unique in the beginning, so they will compute distinct updates and integrate themselves as diverse parts of the full network. With this formulation, every neuron’s weight vector is initialized as a random vector sampled from a multi-dimensional Gaussian, so the neurons point in the random direction in the input space. It is possible and common to initialize the biases to be zero since the asymmetry breaking is provided by the small random numbers in the weights.

The he_uniform initializer [46] method for weight initialization is an important tool for initializing the weights which are used in this research. The he_uniform initialization makes sure the weights are appropriate, keeping the signal in a reasonable range of values through many layers. It tries to make sure the distribution of the inputs to each activation function is zero mean and unit variance. To do this, it assumes that the input data has been normalized to the same distribution. The greater the number of inputs a neuron has, the smaller the initial weights should be, in order to compensate the number of inputs. In a word, the he_uniform initialization method tries to initialize weights with a smarter value, such that neurons won’t start training in saturation.

3.6 Regularization

To reduce overfitting some regularization methods are implemented in neural networks. One of them is L2 regularization. L2 regularization is perhaps the most common form of regularization. It can be implemented by penalizing the squared magnitude of all parameters directly in the objective. For every weight w in the network, the term $\frac{1}{2}\lambda w^2$ is added to the objective, where λ is the regularization

strength. It is common to see the factor of $\frac{1}{2}$ in front because then the gradient of this term with respect to the parameter w is simply λw instead of $2\lambda w$. The L2 regularization has the intuitive interpretation of heavily penalizing peaky weight vectors and preferring diffuse weight vectors.

L1 regularization is another relatively common form of regularization, where for each weight w we add the term $\lambda|w|$ to the objective. It is possible to combine the L1 regularization with the L2 regularization: $\lambda_1 w + \lambda_2 w^2$ (this is called Elastic net regularization [47]). The L1 regularization has the intriguing property that it leads the weight vectors to become sparse during optimization (i.e. very close to exactly zero). In other words, neurons with L1 regularization end up using only a sparse subset of their most important inputs and become nearly invariant to the “noisy” inputs. In comparison, final weight vectors from L2 regularization are usually diffuse, small numbers.

Another form of regularization is to enforce an absolute upper bound on the magnitude of the weight vector for every neuron and use projected gradient descent to enforce the constraint. This is known as max norm constraints.

Dropout is an extremely effective, simple and recently introduced regularization technique [48]. While training, dropout is implemented by only keeping a neuron active with some probability p (a hyperparameter), or setting it to zero otherwise. During training, Dropout can be interpreted as sampling a Neural Network within the full Neural Network, and only updating the parameters of the sampled network based on the input data. (However, the exponential number of possible sampled networks are not independent because they share the parameters.) During testing, there is no dropout applied, with the interpretation of evaluating an averaged prediction across the exponentially-sized ensemble of all sub-networks. Figure 3.4 illustrates the dropout idea where cross means that the neurons are set to zero (randomly).

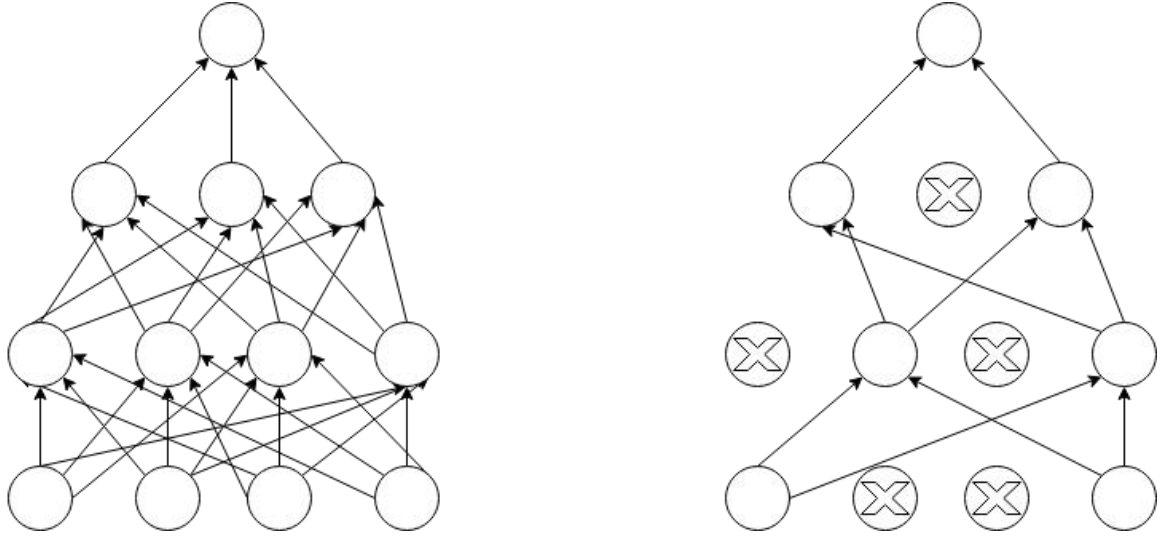


Figure 3.4: Dropout used in a network

3.7 Loss Function

The data loss, which is a supervised learning problem measures the compatibility between a prediction (e.g. the class scores in classification) and the ground truth label. The data loss takes the form of an average over the data losses for every individual example. That is, $L = \frac{1}{N} \sum L_i$ where N is the number of training data and $f = f(x_i; W)$.

If the correct output y_i is a binary vector where every example may or may not have a certain attribute. In this case, the way is to build a binary classifier for every single attribute independently. For example, a binary classifier for each category independently would take the form:

$$L_i = \sum \max(0, 1 - y_{ij} f_j) \quad (4)$$

where the sum is over all categories j , and y_{ij} is either +1 or -1 depending on whether the i th example is labeled with the j th attribute, and the score vector f_j will be positive when the class is predicted to be present and negative otherwise. Notice that loss is accumulated if a positive example has a score less than +1, or when a negative example has a score greater than -1.

3.8 Learning

How the neural network learns through iteration and updates its weights to minimize the loss function will now be discussed.

3.8.1 Backpropagation

When training the network there are mostly two passes which need to be completed one after another. The forward pass computes values from inputs to output and the backward pass then performs backpropagation which starts at the end and recursively applies the chain rule to compute the gradients all the way to the inputs of the circuit. The Backpropagation algorithm is used to learn the weights of a multilayer neural network with a fixed architecture. It performs gradient descent to try to minimize the sum squared error between the network's output values and the given target values.

Figure 3.5 explains (depicted as a lined pattern) at the output node and activation (depicted as a solid pattern) at the hidden node. While the change to an input to hidden weight depends on the error at the hidden node (which in turn depend on the error at all the output nodes) and activation at the input node.

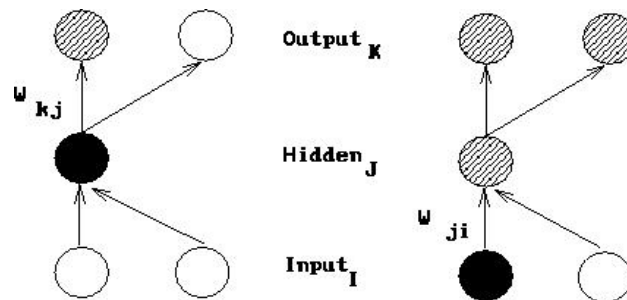


Figure 3.5: The change to a hidden to output weight depends on error [42]

For the purpose of this derivation:

- The subscript k denotes the output layer.
- The subscript j denotes the hidden layer.
- The subscript i denotes the input layer.
- w_{kj} denotes a weight from the hidden to the output layer.
- w_{ji} denotes a weight from the input to the hidden layer.

- a denotes an activation value (sigmoid function).
- t denotes a target value.
- net denotes the net input.

The total error in a network is given by the following equation:

$$E = \frac{1}{2} \sum (t_k - a_k)^2 \quad (5)$$

We want to adjust the network's weights to reduce this overall error.

$$\Delta W \propto - \frac{\partial E}{\partial W} \quad (6)$$

We will begin at the output layer with a particular weight.

$$\Delta W_{kj} \propto - \frac{\partial E}{\partial W_{kj}} \quad (7)$$

However, the error is not directly a function of a weight. We expand this as follows.

$$\Delta W_{kj} = - \epsilon \frac{\partial E}{\partial a_k} \frac{\partial a_k}{\partial net_k} \frac{\partial net_k}{\partial W_{kj}} \quad (8)$$

Let's consider each of these partial derivatives in turn. Note that only one term of the E summation will have a non-zero derivative: the one associated with the particular weight we are considering.

Derivative of the error with respect to the activation:

$$\frac{\partial E}{\partial a_k} = \frac{\partial (\frac{1}{2} \sum (t_k - a_k)^2)}{\partial a_k} = - (t_k - a_k) \quad (9)$$

Derivative of the activation with respect to the net input:

$$\frac{\partial a_k}{\partial net_k} = \frac{\partial (1 + e^{-net_k})^{-1}}{\partial net_k} = \frac{e^{-net_k}}{(1 + e^{-net_k})^2} \quad (10)$$

Using the activation function's equation, we can rewrite the result of the partial derivative as:

$$a_k(1 - a_k) \quad (11)$$

Derivative of the net input with respect to a weight:

$$\frac{\partial net_k}{\partial W_{kj}} = \frac{\partial (\sum a_j W_{kj})}{\partial W_{kj}} = a_j \quad (12)$$

Now substituting these results back into our original equation (8), we have:

$$\Delta W_{kj} = \epsilon (t_k - a_k) a_k (1 - a_k) a_j \quad (13)$$

This equation is typically simplified as shown below where the δ term represents the product of the error with the derivative of the activation function.

$$\Delta W_{kj} = \epsilon \delta_k a_j \quad (14)$$

Now we have to determine the appropriate weight change for an input to hidden weight. This is more complicated because it depends on the error at all of the nodes this weighted connection can lead to.

$$\begin{aligned}
\Delta W_{ji} &\propto \left(\sum \frac{\partial E}{\partial a_k} \frac{\partial a_k}{\partial net_k} \frac{\partial net_k}{\partial a_j} \right) \frac{\partial a_j}{\partial net_j} \frac{\partial net_j}{\partial W_{ji}} \\
&= \epsilon (\sum (t_k - a_k) a_k (1 - a_k) W_{kj}) a_j (1 - a_j) a_i \\
&= \epsilon (\sum \delta_k W_{kj}) a_j (1 - a_j) a_i
\end{aligned}$$

So, the final form it takes: $\Delta W_{ji} = \epsilon \delta_j a_i$ (15)

3.8.2 Gradient Checks

Performing a gradient check is as simple as comparing the analytic gradient to the numerical gradient. The centered difference formula of the form or the finite difference approximation when evaluating the numerical gradient looks as follows:

$$\frac{df(x)}{dx} = \frac{f(x+h) - f(x-h)}{2h} \quad (16)$$

This requires us to evaluate the loss function twice to check every single dimension of the gradient (so it is about 2 times as expensive), but the gradient approximation turns out to be much more precise. To see this, Taylor expansion of $f(x+h)$ and $f(x-h)$ is used which also verifies that the first formula has an error on order of $O(h)$, while the second formula only has error terms on order of $O(h^2)$.

For comparing the numerical gradient f'_n and analytic gradient f'_a , introducing the relative error:

$$\frac{|f'_a - f'_n|}{\max(|f'_a|, |f'_n|)} \quad (17)$$

Which considers their ratio of the differences to the ratio of the absolute values of both gradients. In practice:

- relative error $> e^{-2}$ usually means the gradient is probably wrong
- $e^{-2} > \text{relative error} > e^{-4}$ should be okay.
- $e^{-4} > \text{relative error}$ is usually okay for objectives with kinks (Kinks refer to non-differentiable parts of an objective function). But if there are no kinks (e.g. use of tanh nonlinearities and softmax), then e^{-4} is too high.
- e^{-7} and less should be great.

3.8.3 Learning Rate

The rate the weights will be updated is known as the learning rate for the model. The learning rate needs to be controlled as the effects of different learning rates can produce different results and the goal is to minimize the loss function. This is depicted in figure 3.5 as with low learning rates the improvements will be linear. With high learning rates, they will start to look more exponential. Higher learning rates will decay the loss faster, but they get stuck at worse values of loss (green line). This is because there is too much "energy" in the optimization and the parameters are bouncing around chaotically, unable to settle in a nice spot in the optimization landscape.

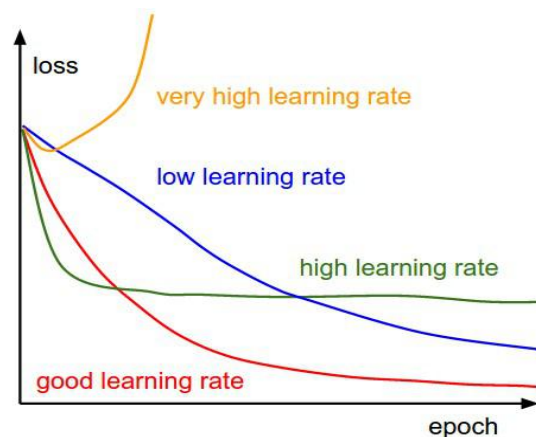


Figure 3.6: Loss function is changing with different learning rates [42]

3.8.4 Per-Parameter Adaptive Learning Rate Methods

All previous approaches we've discussed so far manipulated the learning rate globally and equally for all parameters. Tuning the learning rates is an expensive process, so much work has gone into devising methods that can adaptively tune the learning rates, and even do so per parameter. Many of these methods may still require other hyperparameter settings, but the argument is that they are well-behaved for a broader range of hyperparameter values than the raw learning rate. In this section, we highlight some common adaptive methods.

Adagrad:

Adagrad is an adaptive learning rate method originally proposed by Duchi et al [49]. In the Adagrad method, the denominator accumulates the squared gradients from each iteration starting at the beginning of training. Since each term is positive, this

accumulated sum continues to grow throughout training, effectively shrinking the learning rate on each dimension. In this method, the variable cache has the size equal to the size of the gradient and keeps track of the per-parameter sum of squared gradients. This is then used to normalize the parameter update step, element-wise. The weights that receive high gradients will have their effective learning rate reduced, while weights that receive small or infrequent updates will have their effective learning rate increased. The smoothing term “eps” (usually set somewhere in the range from e^{-4} to e^{-8}) avoids division by zero. A downside of Adagrad is that in the case of Deep Learning, the monotonic learning rate usually proves too aggressive and stops learning too early.

Adadelta:

Adadelta is a more robust extension of Adagrad that adapts learning rates based on a moving window of gradient updates, instead of accumulating all past gradients [50]. This way, Adadelta continues learning even when many updates have been done. The method dynamically adapts over time using only first order information and has minimal computational overhead beyond vanilla stochastic gradient descent.

After many iterations, this learning rate will become infinitesimally small. The method requires no manual tuning of a learning rate and appears robust to noisy gradient information, different model architecture choices, various data modalities, and selection of hyperparameters.

The two main drawbacks of Adagrad which were improved in Adadelta:

- The continual decay of learning rates throughout training
- The need for a manually selected global learning rate.

3.9 Conclusion

Neural network tries to mimic the construction of the human optical system. It is generally consisted of three layers. At first, some minimal data processing is done and the weights are initialized of the network. Then the network is ready to train and the gradient is calculated so the weights can be changed in such a way that the loss of the network will be minimized.

CHAPTER 4

Convolutional Neural Networks (CNN)

This chapter discussed in detail about convolutional neural network. It explores the architecture of CNN and how it works to solve a problem.

4.1 CNN

Convolutional Neural Networks (CNN) are very similar to the ordinary Neural Network discussed before. CNN is also made up of neurons that have learnable weights and biases. Each neuron receives some inputs, performs a dot product and optionally follows it with a non-linearity. The whole network expresses a single differentiable score function: from the raw image pixels on one end to class scores at the other. And they have a loss function (e.g. SVM/Softmax) on the last (fully-connected) layer just like an ordinary neural network. The main difference is ConvNet architectures make the explicit assumption that the inputs are images, which allows the model to encode certain properties into the architecture. These then make the forward function more efficient to implement and vastly reduce the number of parameters in the network.

CNN is a trainable deep learning architecture. This was encouraged by animal optical system [45] that learns features directly from the given input data avoiding the hand-crafted feature. CNN consists of multiple nonlinear transformations in several steps and in each step, it works to reduce the error to accurately classify. In summary, a CNN is made of multiple trainable stages composed like a stack of data top of each other followed by a supervised classifier. Each stage has a set of arrays named feature vectors which represent the input and output vectors respectively [45]. CNN needs a huge number of labeled samples and computational power to train the network. Because of the growth of the available digital data and powerful computational resources i.e. graphics processing unit (GPU), [51] the required time is being reduced significantly than before while training the network. This convenience can help us to train deeper CNN architectures in our environment to achieve a greater result.

4.2 CNN Architecture

Before further going to the details, let us explain how a CNN network converges. It is a structured neural network which requires minimal preprocessing where the first couple of layers are sequentially interconnected in order to process visual information. CNN is feed-forwarding in nature since the output of the current layer becomes the input of the next layer. Neurons in the CNN have learnable parameters such as weights and biases. The network starts training itself with a forward pass. A list of connected layers transforms the input volume into an output volume. The prediction in the output layer is computed as probability that represents class scores. The predicted outcome is then compared with the true result to compute the error. In backpropagation, the computed error generates the gradient that flows in the backward direction. At each step, the parameters are tuned in such a direction that it tries to reduce the previously generated error [52][53][54]. This process continues in an iterative way until the model converges.

Convolutional Neural Networks take advantage of the fact that the input consists of images and they constrain the architecture in a more sensible way. In particular, unlike a regular Neural Network, the layers of a ConvNet have neurons arranged in 3 dimensions: width, height, depth. (Note that the word depth here refers to the third dimension of an activation volume, not to the depth of a full Neural Network, which can refer to the total number of layers in a network.) The neurons in a layer will only be connected to a small region of the layer before it, instead of all of the neurons in a fully-connected manner. A ConvNet is made up of Layers. Every Layer has a simple API: It transforms an input 3D volume to an output 3D volume with some differentiable function that may or may not have parameters. Figure 4.1 depicts this ConvNet process. From the figure, (Top) A regular 3-layer Neural Network. (Bottom) A ConvNet arranges its neurons in three dimensions (width, height, depth), as visualized in one of the layers. Every layer of a ConvNet transforms the 3D input volume to a 3D output volume of neuron activations. In this example, the red input layer holds the image, so its width and height would be the dimensions of the image, and the depth would be 3 (Red, Green, Blue channels).

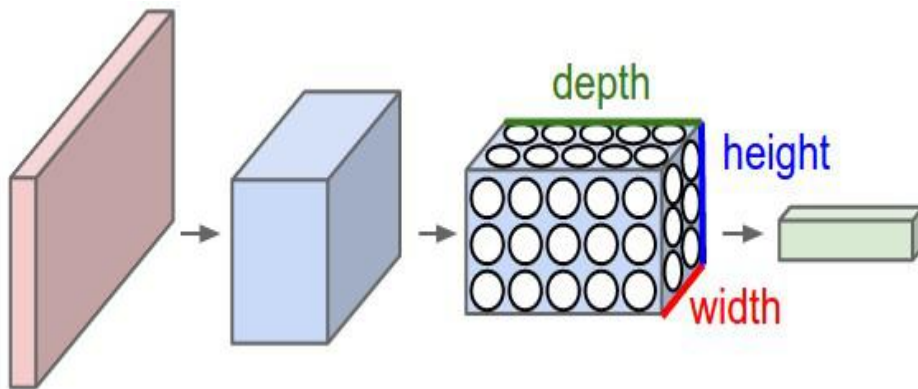
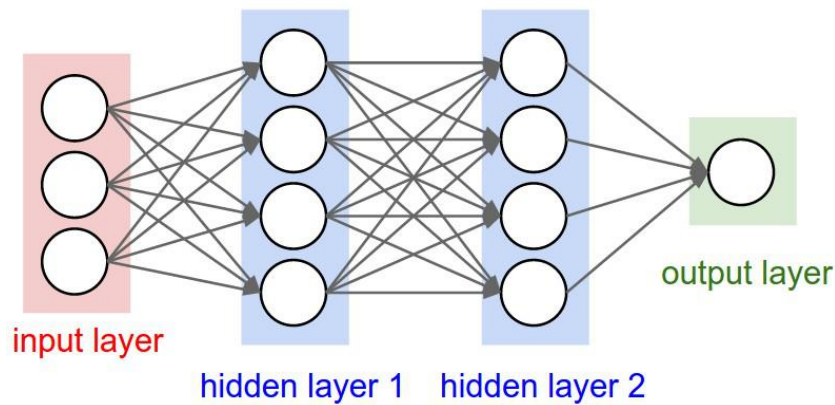


Figure 4.1: Comparison of an original Neural Network with a CNN [42]

4.3 Layers in CNN

A simple ConvNet is a sequence of layers, and every layer of a ConvNet transforms one volume of activations to another through a differentiable function. Three main types of layers are needed to build ConvNet architectures: Convolutional Layer, Pooling Layer, and Fully-Connected Layer (exactly as seen in regular Neural Networks). Stack these layers together to form a full ConvNet architecture. Figure 4.2 shows how a typical CNN architecture looks like.

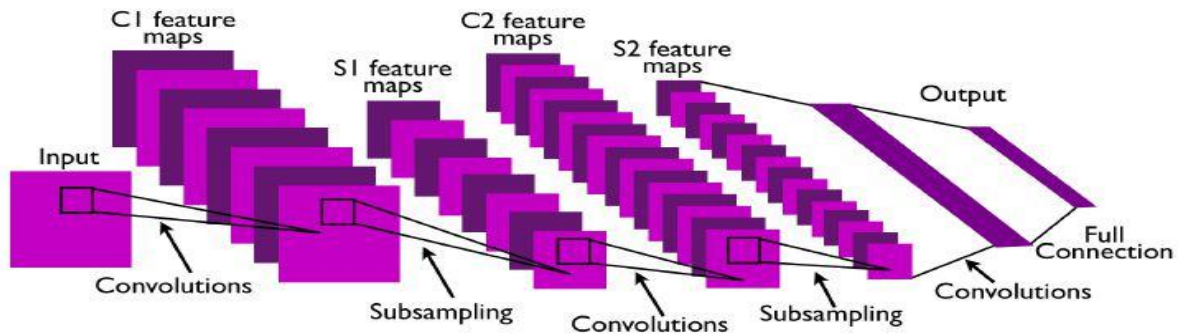


Figure 4.2: A typical CNN architecture [45]

Figure 4.3 describes the activations of an example ConvNet architecture. The initial volume stores the raw image pixels (left) and the last volume stores the class scores (right). Each volume of activations along the processing path is shown as a column. Since it's difficult to visualize 3D volumes, we lay out each volume's slices in rows. The last layer volume holds the scores for each class, but here we only visualize the sorted top 5 scores and print the labels of each one.

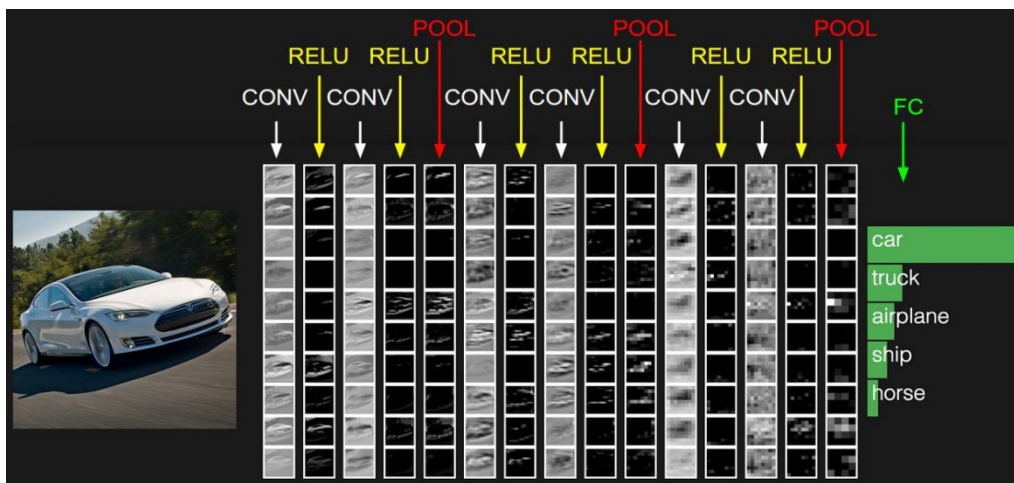


Figure 4.3: ConvNet architecture example [42]

4.3.1 Convolutional Layer

The Conv layer is the core building block of a Convolutional Network that does most of the computational heavy lifting. The CONV layer's parameters consist of a set of learnable filters. Every filter is small spatially (along width and height), but extends through the full depth of the input volume. For example, a typical filter on the first layer of a ConvNet might have size $5 \times 5 \times 3$ (i.e. 5 pixels width and height, and 3

because images have depth 3, the color channels). During the forward pass, each filter is slid i.e. convolved across the width and height of the input volume and compute dot products between the entries of the filter and the input at any position.

As we slide the filter over the width and height of the input volume we will produce a 2-dimensional activation map that gives the responses of that filter at every spatial position shown in figure 4.4. Intuitively, the network will learn filters that activate when they see some type of visual features such as an edge of some orientation or a blotch of some color on the first layer, or eventually entire honeycomb or wheel-like patterns on higher layers of the network. Now, we will have an entire set of filters in each CONV layer (e.g. 12 filters), and each of them will produce a separate 2-dimensional activation map. We will stack these activation maps along the depth dimension and produce the output volume.

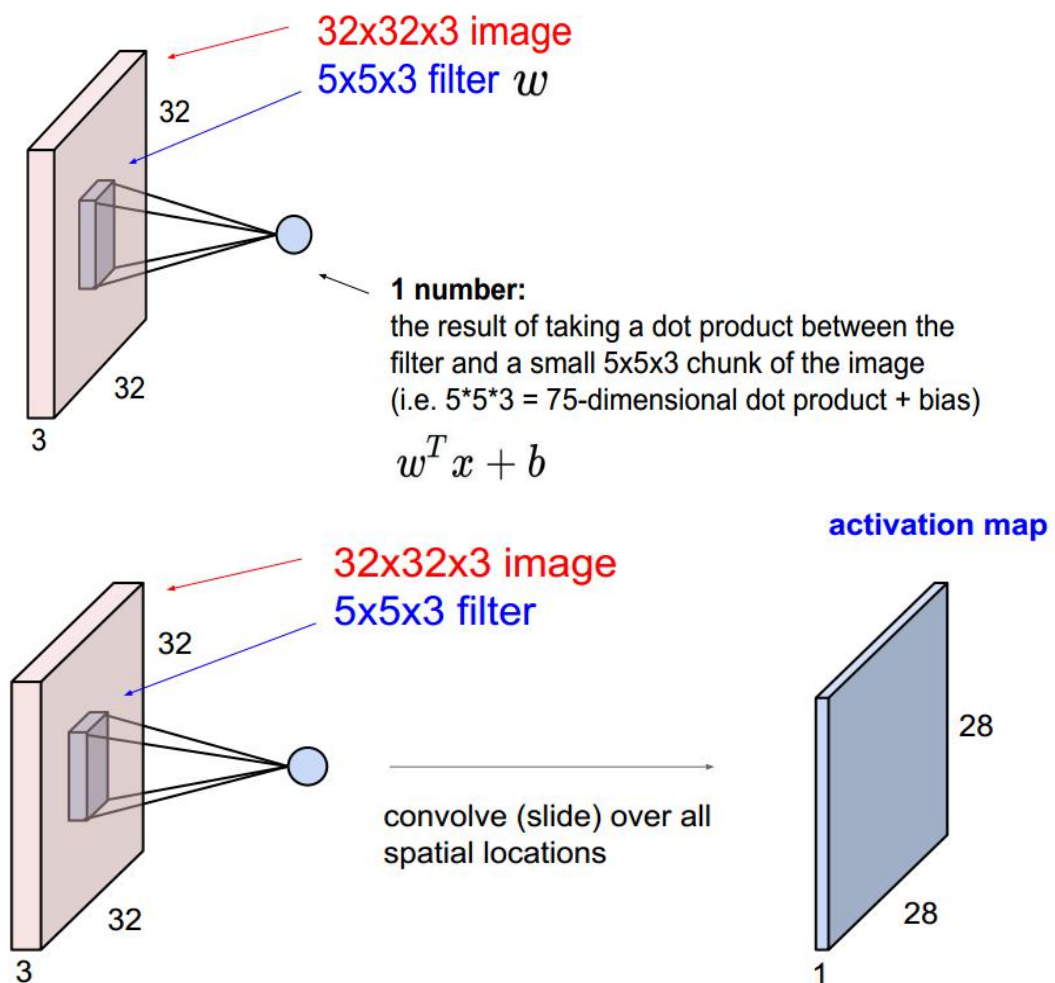


Figure 4.4: Convolution layer example [42]

An example in figure 4.5 shows (Top) an input volume in red (e.g. a 32x32x3 CIFAR-10 image), and an example volume of neurons in the first Convolutional layer. Each neuron in the convolutional layer is connected only to a local region in the input volume spatially but to the full depth (i.e. all color channels). There are multiple neurons (5 in this example) along the depth, all looking at the same region in the input. (Bottom) The neurons from the Neural Network chapter remain unchanged: They still compute a dot product of their weights with the input followed by a non-linearity, but their connectivity is now restricted to be local spatially.

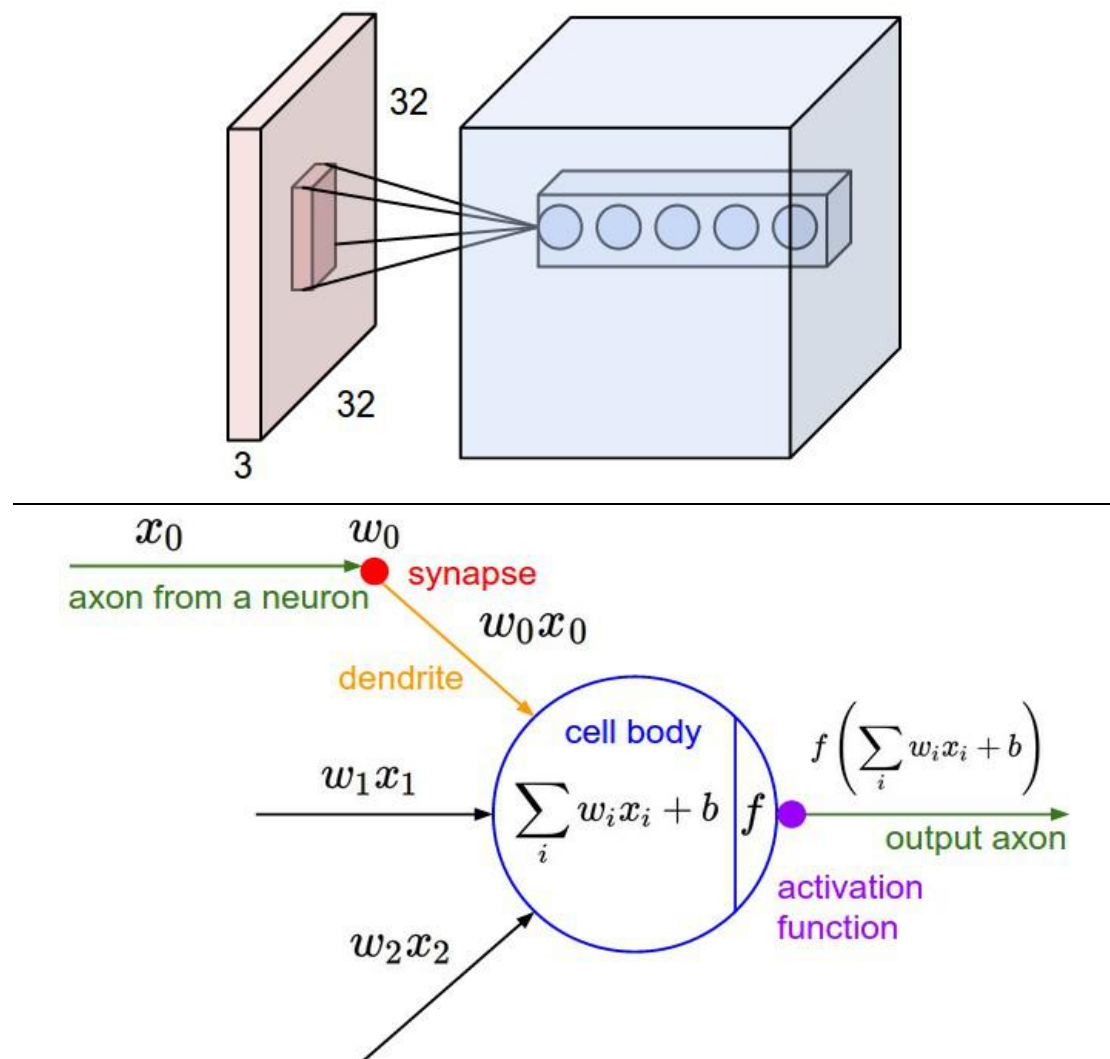


Figure 4.5: Example of local connectivity [42]

Three hyperparameters control the size of the output volume: the depth, stride, and zero-padding. The depth of the output volume is a hyperparameter: it corresponds

to the number of filters that are being used to each learning to look for something different in the input. The number of the stride must be specified with which we slide the filter. When the stride is 1 then we move the filters one pixel at a time. When the stride is 2 (or uncommonly 3 or more, though this is rare in practice) then the filters jump 2 pixels at a time as we slide them around. This will produce smaller output volumes spatially. Finally, sometimes it will be convenient to pad the input volume with zeros around the border. The size of this zero-padding is a hyperparameter. The nice feature of zero padding is that it will allow us to control the spatial size of the output volumes.

The spatial size of the output volume can be computed as a function of the input volume size (W), the receptive field size of the Conv Layer neurons (F), the stride with which they are applied (S) and the amount of zero padding used (P) on the border. In general, setting zero padding to be $P = \frac{F-1}{2}$ when the stride is $S = 1$ ensures that the input volume and output volume will have the same size spatially.

4.3.2 Activation Layer

The activation layer introduces non-linear properties to the network followed by convolution layers. Their main purpose is to convert an input signal of a node into an output signal. The generated output will be passed towards the next layer. Every activation function (or non-linearity) takes a single number and performs a certain fixed mathematical operation on it. There are many activation functions to choose from. Two activation functions are discussed here.

Sigmoid: The sigmoid non-linearity has the mathematical form $\sigma(x) = \frac{1}{1+e^{-x}}$ and is shown in figure 4.6. It takes a real-valued number and “squashes” it into a range between 0 and 1. In particular, large negative numbers become 0 and large positive numbers become 1. The sigmoid function has seen frequent use historically since it has a nice interpretation as the firing rate of a neuron: from not firing at all (0) to fully-saturated firing at an assumed maximum frequency (1).

(i) In practice, the sigmoid non-linearity has recently fallen out of favor and it is rarely ever used. It has two major drawbacks:

- (ii) A very undesirable property of the sigmoid neuron is that when the neuron's activation saturates at either tail of 0 or 1, the gradient at these regions is almost zero. Therefore, if the local gradient is very small, it will effectively “kill” the gradient and almost no signal will flow through the neuron to its weights and recursively to its data.
- (iii) Sigmoid outputs are not zero-centered. This is undesirable since neurons in later layers of processing in a Neural Network (more on this soon) would be receiving data that is not zero-centered.

ReLU: The Rectified Linear (ReLU) Unit has become very popular in the last few years. It is computationally efficient and converges much faster than most other activation functions [14]. It computes the function $f(x) = \max(0, x)$ showed in figure 4.7. In other words, the activation is simply being the threshold at zero (see image above on the left). There are several pros and cons to using the ReLUs:

- (i) It was found to greatly accelerate the convergence of stochastic gradient descent compared to the sigmoid functions.
- (ii) Compared to sigmoid neurons that involve expensive operations (exponentials, etc.), the ReLU can be implemented by simply thresholding a matrix of activations at zero.
- (iii) Unfortunately, ReLU units can be fragile during training and can “die”. For example, a large gradient flowing through a ReLU neuron could cause the weights to update in such a way that the neuron will never activate on any datapoint again. If this happens, then the gradient flowing through the unit will forever be zero from that point on. That is, the ReLU units can irreversibly die during training since they can get knocked off the data manifold.
- (iv) Compared to sigmoid neurons that involve expensive operations (exponentials, etc.), the ReLU can be implemented by simply thresholding a matrix of activations at zero.
- (v) Unfortunately, ReLU units can be fragile during training and can “die”. For example, a large gradient flowing through a ReLU neuron could cause the weights to update in such a way that the neuron will never activate on any datapoint again. If this happens, then the gradient flowing through the unit will forever be zero from that point on. That is, the ReLU units can irreversibly die during training since they can get knocked off the data manifold.

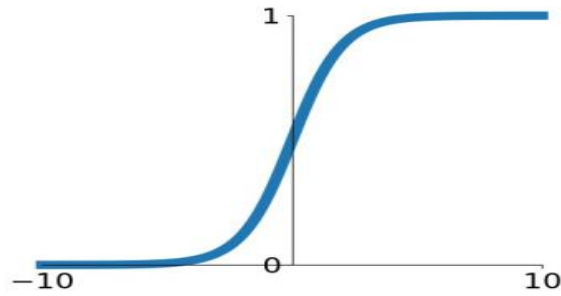


Fig 4.6: Activation function: tanh

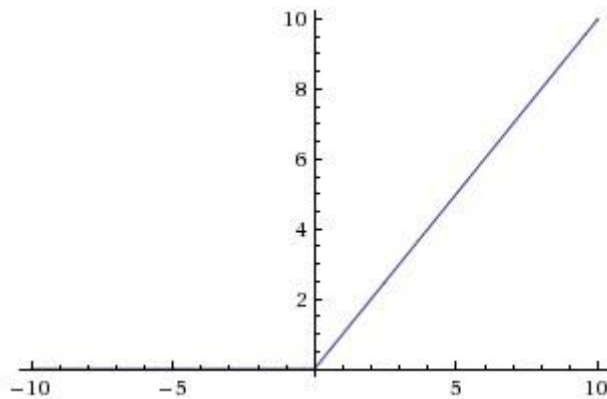


Figure 4.7: Activation function: ReLU

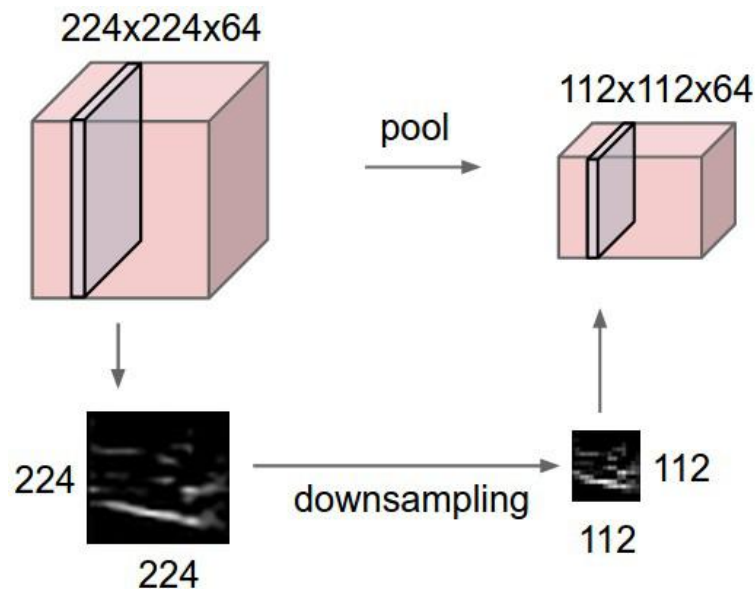
4.3.3 Pooling Layer

It is common to periodically insert a Pooling layer in-between successive Conv layers in a ConvNet architecture. Its function is to progressively reduce the spatial size of the representation to reduce the number of parameters and computation in the network, and hence to also control overfitting. The Pooling Layer operates independently on every depth slice of the input and resizes it spatially, using the MAX operation. The most common form is a pooling layer with filters of size 2x2 applied with a stride of 2 downsamples every depth slice in the input by 2 along both width and height, discarding 75% of the activations. Every MAX operation would, in this case, be taking a max over 4 numbers (little 2x2 region in some depth slice). The depth dimension remains unchanged. More generally, the pooling layer:

- Accepts a volume of size $W_1 * H_1 * D_1$
- Requires two hyperparameters:
 - their spatial extent F ,
 - the stride S ,

- Produces a volume of size $W_2 * H_2 * D_2$ where:
 - $W_2 = \frac{W_1 - F}{S} + 1$
 - $H_2 = \frac{H_1 - F}{S} + 1$
 - $D_2 = D_1$
- Introduces zero parameters since it computes a fixed function of the input
- For Pooling layers, it is not common to pad the input using zero-padding.

Pooling layer downsamples the volume spatially, independently in each depth slice of the input volume. In this example of figure 4.8, (top) the input volume of size $[224 \times 224 \times 64]$ is pooled with filter size 2, stride 2 into output volume of size $[112 \times 112 \times 64]$. Notice that the volume depth is preserved. (Bottom) The most common downsampling operation is max, giving rise to max pooling, here shown with a stride of 2. That is, each max is taken over 4 numbers (little 2×2 square).



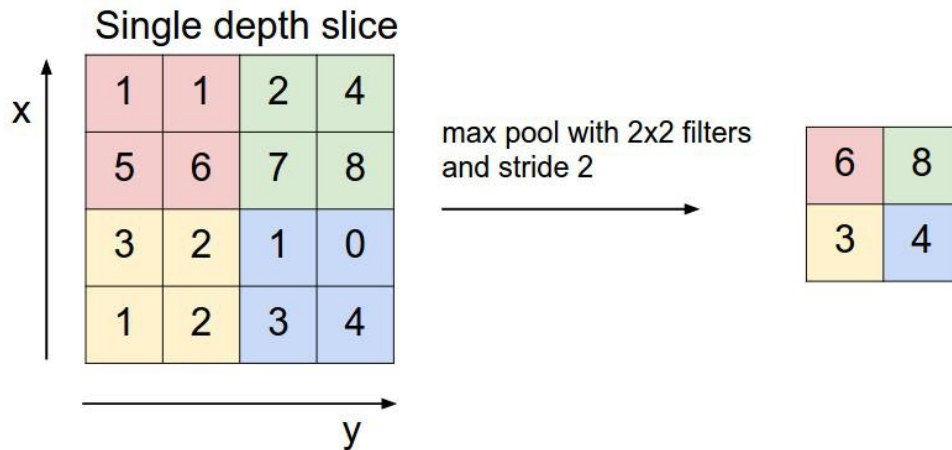


Figure 4.8: Example of maxpooling [42]

4.3.4 Fully-Connected (FC) Layer

Neurons in a fully connected layer have full connections to all activations in the previous layer, as seen in regular Neural Networks. Their activations can hence be computed with a matrix multiplication followed by a bias offset. It is worth noting that the only difference between FC and CONV layers is that the neurons in the CONV layer are connected only to a local region in the input and that many of the neurons in a CONV volume share parameter. However, the neurons in both layers still compute dot products, so their functional form is identical. Therefore, it turns out that it's possible to convert between FC and CONV layers:

- For any CONV layer, there is an FC layer that implements the same forward function. The weight matrix would be a large matrix that is mostly zero except for at certain blocks (due to local connectivity) where the weights in many of the blocks are equal (due to parameter sharing).

Conversely, any FC layer can be converted to a CONV layer. For example, an FC layer with $K=4096$ that is looking at some input volume of size $7 \times 7 \times 512$ can be equivalently expressed as a CONV layer with $F=7, P=0, S=1, K=4096$. In other words, we are setting the filter size to be exactly the size of the input volume, and hence the output will simply be $1 \times 1 \times 4096$ since only a single depth column “fits” across the input volume, giving an identical result as the initial FC layer.

The final fully connected layer of the network produces the net output with an activation function i.e. softmax function depending on the number of classes in the classification problem.

A typical CNN architecture consists of these types of several components. An example of a typical architecture would be:

$$[(\text{CONV-RELU}) * N - \text{POOL}] * M - (\text{FC-RELU}) * K, \text{SOFTMAX}$$

where N is usually up to ~ 5 , M is large, $0 \leq K \leq 2$.

4.4 Known Architectures in CNN

There are several architectures in the field of Convolutional Networks that have a name. The most common are:

- **LeNet:** The first successful applications of Convolutional Networks were developed by Yann LeCun in 1990's. Of these, the best known is the LeNet architecture [34] that was used to read zip codes, digits, etc.
- **AlexNet:** The first work that popularized Convolutional Networks in Computer Vision was the AlexNet [14], developed by Alex Krizhevsky, Ilya Sutskever and Geoff Hinton. The Network had a very similar architecture to LeNet, but was deeper, bigger, and featured Convolutional Layers stacked on top of each other (previously it was common to only have a single CONV layer always immediately followed by a POOL layer).
- **GoogLeNet:** The ILSVRC (Large Scale Visual Recognition Challenge) 2014 winner was a Convolutional Network from Szegedy et al. [47] from Google. Its main contribution was the development of an Inception Module that dramatically reduced the number of parameters in the network (4M, compared to AlexNet with 60M). Additionally, this paper uses Average Pooling instead of Fully Connected layers at the top of the ConvNet, eliminating a large number of parameters that do not seem to matter much.
- **VGGNet:** The runner-up in ILSVRC 2014 was the network from Karen Simonyan and Andrew Zisserman that became known as the VGGNet [48]. Its main contribution was in showing that the depth of the network is a critical component for good performance. Their final best network contains 16 CONV/FC layers and, appealingly, features an extremely homogeneous

architecture that only performs 3x3 convolutions and 2x2 pooling from the beginning to the end.

- **ResNet:** Residual Network developed by Kaiming He et al. [49] was the winner of ILSVRC 2015. It features special skip connections and a heavy use of batch normalization. The architecture is also missing fully connected layers at the end of the network. The reader is also referred to Kaiming's presentation (video, slides), and some recent experiments that reproduce these networks in Torch. ResNets are currently by far state of the art Convolutional Neural Network models and are the default choice for using ConvNets in practice.

4.5 Conclusion

CNN is another form of the ordinary neural network but it takes images as inputs. CNN architectures are mainly constructed by some major layers and they are stacked one after another.

Chapter 5

Methodology

This chapter consists of the work flow throughout the research. It includes data collection, building databank for training and validation set, developing deep CNN for training, classifying crack and non crack images.

5.1 Data Source

The datasets are collected [55]. The datasets contains images of various concrete surfaces including cracks and non cracks. The image data are divided into two as negative(non crack) and positive(crack) in separate folder for classifying images. Each class contains 20000 images with a total of 40000 images with 227 x 227 x 3 pixels (RGB). No data augmentation is applied.

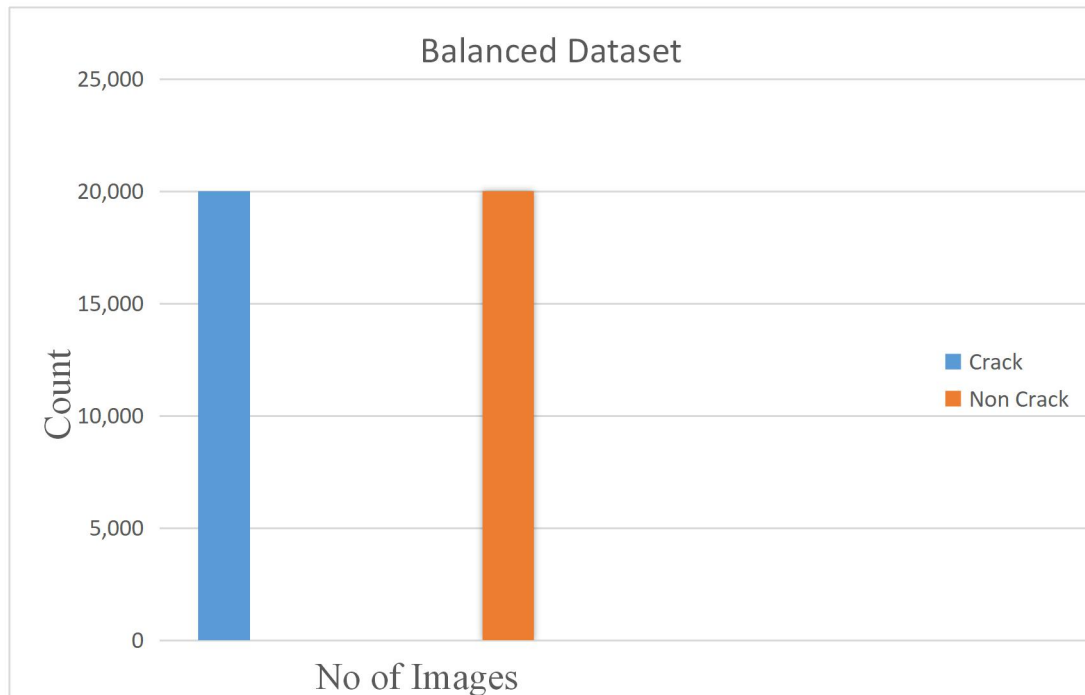


Fig 5.1 No of Crack and Non crack images

So the number of positive and negative images is same. All the images are in JPG format. Figure 5.2 some crack and non crack images sample from dataset.



Fig 5.2: Non Crack and Crack Images [55]

5.1.2 Data Preprocessing:

As mentioned earlier we have a large number of dataset (40,000). Feeding this number dataset in to CNN will increase the complexity and computational time. To reduce computational time and complexity the images are reshaped into 150 x 150 pixels. And after that the images are again rescaled by multiplying each pixel with (1/255). Randomly 2000 images were taken for validation. And the rest were used for training the architecture. Figure 5.3 shows a crack reshaped image.



227 x 227 pixel crack image



150 x 150 pixel crack image

Fig 5.3: Example of a reshaped crack image

5.2 Model Architecture and Training

The implemented architecture consists of 6 convolutional layers where maxpooling layer was inserted after each convolutional layer which is shown in figure 8.4. The number of 256 filters of different sizes is used in each convolutional layers. For example, 1x1 size was used in convolution 1, 2, 3 and 6. 3x3 filter is used in convolution 4 and 5. ReLU non linearity was used in each convolution layer. Three hidden dense layer was used in the fully connected layer. The final fully connected layer consists of only one neuron with “sigmoid” non-linearity to produce the class score.

The weights are initialized with ‘he_uniform’ initialization method [46]. It draws samples from a uniform distribution within [-limit, limit], where $\text{limit} = \sqrt{6 / \text{fan_in}}$ (fan_in is the number of input units in the weight tensor). . The network is trained all over using Adam optimizer with initial standard parameters. The model is trained with mini batches of size 64. Figure 5.4 shows the architecture of implemented convolutional neural network. No data augmentation was needed. Besides binary cross entropy loss function was used.

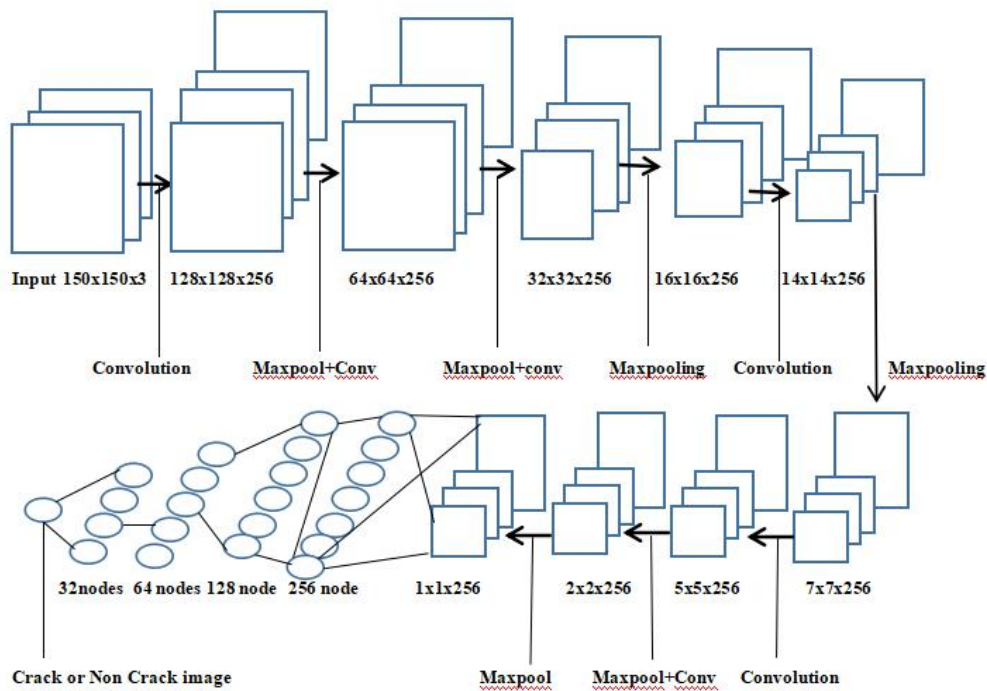


Fig 5.4: The architecture of implemented CNN

From the figure we can see the input of the first layer was 150x150x3. In each layer 256 filters were used. It was initialized with 'he_uniform' kernel initializer. 6 convolutional layers were used. After that, fully connected layer was added. The final output was 1 node that indicates either a crack or non crack image. When the model was implemented completely, several crack or non crack images were tested. Table 5.1 shows the model summary.

Table 5.1 Model Summary

Layer(Type)	Output Shape	No of Parameter
Input	(150, 150, 3)	0
Convolution1	(128, 128, 256)	1024
Maxpooling	(64, 64, 256)	0
Convolution2	(64, 64, 256)	65792

Maxpooling	(32, 32, 256)	0
Convolution3	(32, 32, 256)	65792
Maxpooling	(16, 16, 256)	0
Convolution4	(14, 14, 256)	590080
Maxpooling	(7, 7, 256)	0
Convolution5	(5, 5, 256)	590080
Maxpooling	(2, 2, 256)	0
Convolution6	(2, 2, 256)	65792
Maxpooling	(1, 1, 256)	0
Flatten	(256, 1)	0
Dense	(128, 1)	32896
Dense	(64, 1)	8256
Dense	(32, 1)	2080
Sigmoid	(1)	33

The crack detection is a binary classification task. The output is a binary label $y \in \{0,1\}$; representing the absence of crack or not respectively. In the training set, weighted binary cross entropy loss is optimized. The loss is defined as:

$$CE = -\sum_i^c t_i \log(s_i)$$

Where t_i and s_i are the groundtruth and the CNN score for each class i in C . As usually an activation function (Sigmoid / Softmax) is applied to the scores before the CE Loss computation, we write $f(s_i)$ to refer to the activations [56].

5.3 Conclusion

The chapter is about building a deep CNN architecture. A number of total 1,421,825 parameters are used.

CHAPTER 6

Results and Performance Analysis

6.1 Environment

The CNN model was trained in kaggle notebook [57]. The notebook editing session allows 9 hours execution time. It has 20 Gigabytes of auto saved disk including 4 CPU cores, 16 Gigabytes of RAM. And the GPU specs with 2 CPU cores and 13 Gigabytes of RAM. It provides NVIDIA Tesla P100. Keras API on top of TensorFlow (CUDA toolkit 9.0, cuDNN SDK v7 and python 3.6) were used [58].

6.2 Experimental Analysis

The data set is divided into training and validation set randomly. 2000 images are selected for validation and the rest for training. The results presented in this work is based on accuracy and f1 score [59] which are described by the following equations:

$$accuracy = \frac{tp+tn}{tp+tn+fp+fn} \quad (20)$$

$$f1\ score = 2 * \frac{precision*recall}{precision+recall} \quad (21)$$

Where tp, tn, fp, fn represent true positive, true negative, false positive and false negative respectively. Recall is defined as the fraction of the relevant instances in a dataset that is successfully retrieved and precision expresses the proportion of the data points the model says is relevant actually are relevant.

CNN has the advantage of learning features automatically instead of manual feature extraction techniques. The self-learning ability of CNN model makes it more convenient than the traditional learning system. Figure 6.1 shows annotated concrete crack images.

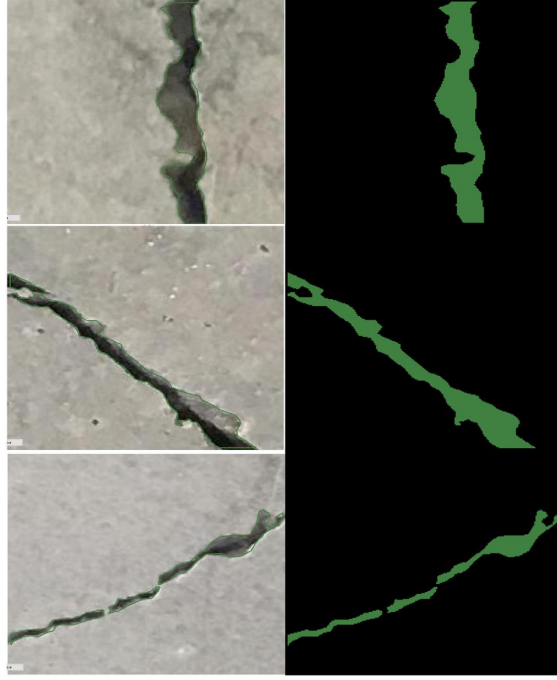


Fig 6.1: Example of annotated concrete crack images [60]

From the figure we can see, cracks are segmented by feature extraction method of CNN. The accuracy curve for the training set (38000 images) and validation set (2000 images) is showed in figure 6.2 for 50 epochs.

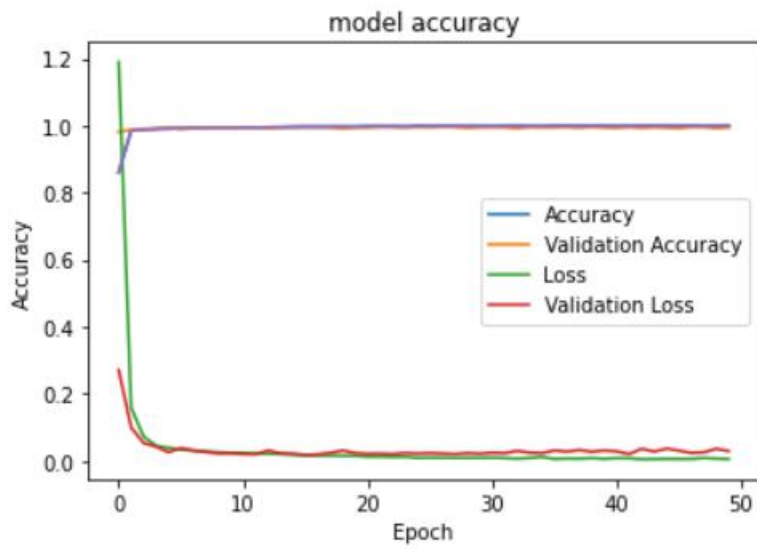


Figure 6.2: Accuracy curve for training and validation

From the figure we can see, by the increasing number of epochs the proposed model gets more accuracy with a decreasing factor of loss. It took around 233s for first epoch and gradually the time was minimized. Using equations (20) and (21), the

proposed system achieved 99.45% accuracy and 99.43% f1 score(validation) which outperformed the previous state of the art which is shown in table 6.1. A recent research [10] had the validation accuracy of 99.39%. Another more recent research [11] had an accuracy of 99.98% using VGG16 and InceptionV3 classifiers.

Table 6.: The proposed system achieved the state of the art result:

Accuracy (Validation Set)	F1 Score (Validation Set)
99.45%	99.43%

The reasons behind this accuracy is, 6 convolutional layers were used including maxpooling layer in each. The accuracy of the network highly depends on the depth of CNN architecture [60]. ‘ReLU’ activation was used in convolutional layer. ‘ReLU’ is computationally efficient and converges much faster than most other activation functions [14]. It computes the function $f(x) = \max(0, x)$ and the activation being threshold at zero. Compared to ‘Sigmoid’ function which has exponential operations ‘ReLU’ can be implemented by simply thresholding a matrix of activation at zero.

The kernels are initialized with ‘he_uniform’ kernel initializer [46]. It simply draws samples from a uniform distribution within [-limit, limit]. Where,

$$limit = \sqrt{6/fan_in} \quad (23)$$

Where fan_in is the number of input units in the weight tensor. So the kernels were also balanced. Three ‘fully connected’ layers were used in the network. To reduce the overfitting L2 regularization was used. It can be applied by explicitly penalizing the square magnitude of all parameters in the target. For every weight w in the network, the term $\frac{1}{2}\lambda w^2$ is added to the objective, where λ is the regularization strength. It regularizes the parameters that constrain, regularizes or shrinks the coefficient estimates towards zero.

‘Sigmoid’ function was used in output layer. The network was trained with Adam optimizer with initial standard parameters. Adam is an optimization algorithm that can be used instead of the classical stochastic gradient descent procedure to update network weights iterative based in training data [61]. As I used a large number of data

and parameters (1,421,825) Adam optimizer was well suited for the network. The images were also noisy, so it was appropriate for those problems. And binary cross entropy function was used to reduce to the loss.

6.3 Conclusion

The proposed method achieved a quite good accuracy detecting crack images. This methodology can contribute a lot in detecting cracks in civil engineering sectors.

CHAPTER 7

Conclusion and Future Works

This chapter discusses the summary of thesis work, its limitation and shows future work direction.

7.1 Summary

The motivation of this research work is to build a machine learning image classification model that have a decent accuracy to classify the crack on surface or road. It is very important to identify the cracks of a building or road in civil engineering sectors. Manually detecting cracks is very time consuming and may not also accurate all the time. The proposed method can detect the crack with a decent accuracy. A 40,000 images of crack and non crack were taken for the method. Some of the images were noisy, some of them consists of dust, shadows etc. The proposed method can handle those problems. The images were 227x227 pixels of size with RGB channel. It was reduced to 150x150 pixels with RGB channel to feed the network and reduce the computational time and complexity. Six layers of convolution were used attaching maxpooling layer in each. And three fully connected layers were used. Finally the result of the architecture came quite good with decent accuracy. Future work can explore different architectures using optimized hyperparameters to improve system accuracy.

7.2 Limitations

We worked with only one data source to train our model. With a bigger dataset and more data sources, we would have more variant data samples where the model can be more generalized for detecting cracks. Besides we did not develop any mobile applications for detecting cracks. With the proposed method mobile application can be developed and cracks can be identified.

7.3 Future Work

The plan is to keep working with object recognition and explore other domains related to this. The plan includes:

- We want to work with other object recognition challenges and try to achieve the state of art accuracy in the respective domain.
- We also want to develop:
 - A new hybrid model architecture which would work to recognize objects much better.
 - Ensemble between different models to achieve greater results.
 - Extract additional features and fusion with CNN architecture for better accuracy.
 - More optimized Hyperparameters.

7.4 Conclusion

The work was completed without facing a major problem. It was a success in detecting Cracks of surface.

References

- [1] Yamaguchi, T., Nakamura, S., Saegusa, R., and Hashimoto, S., “Image-based crack detection for real concrete surfaces,” *IEEJ T. Electr. Electr.* 3(1), 128-135 (2010).
- [2] Oliveira, H. and Lobato Correia, P. “Automatic road crack segmentation using entropy and image dynamic thresholding,” *Proc. EUSIPCO 2009*, 622-626 (2009).
- [3] Santhi B., Krishnamurthy G., Siddharth S., Ramakrishnan P.K., “Automatic detection of cracks in pavements using edge detection operator,” *J. Theor. App. Inf. Technol.* 36(2), 199-205 (2012).
- [4] Abdelqader, I., Abudayyeh, O., and Kelly, M. E., “Analysis of edge-detection techniques for crack identification in bridges,” *J. Comput. Civil Eng.* 17(4), 255-263 (2003).
- [5] Yeum, C. M. and Dyke, S. J., “Vision-based automated crack detection for bridge inspection,” *Comput.-Aided Civ. Infrastruct. Eng.* 30(10), 759-770 (2015).
- [6] Liu, S. W., Huang, J. H., Sung, J. C., and Lee, C. C., “Detection of cracks using neural networks and computational mechanics,” *Comput. Methods Appl. Mech. Engrg.* 191(25–26), 2831-2845 (2002).
- [7] Moselhi, O. and Shehab-Eldeen, T., “Classification of defects in sewer pipes using neural networks,” *J. Infrastruct. Syst.* 6(3), 97-104 (2000).
- [8] Lecun, Y., Bengio, Y., and Hinton, G., “Deep learning,” *Nature.* 521(7553), 436 (2015).
- [9] Krizhevsky, A., Sutskever, I., and Hinton, G. E., “ImageNet classification with deep convolutional neural networks,” *International Conference on Neural Information Processing Systems*, 60, 1097-1105 (2012).

- [10] Deng, J., Dong, W., Socher, R., Li, L. J., Li, K., and Li, F. F., “ImageNet: A large-scale hierarchical image database,” *Proc. CVPR 2009*, 248-255 (2009).
- [11] Zhao, X. F., Han, R. C., Yu, Y., Hu, W. T., Jiao, D., Mao, X. Q., Li, M. C., and Ou, J. P., “Smartphone-based mobile testing technique for quick bridge cable–force measurement,” *J. Bridge Eng.* 22(4), 06016012 (2016).
- [12] A. A. Haider, “Traffic jam: The ugly side of Dhaka's development,” [Online], Available: <https://www.thedailystar.net/opinion/society/traffic-jam-the-ugly-side-dhakas-development-1575355>. [Accessed Dec 14, 2019].
- [13] K. Mahmud, K. Gope, S. Mustafizur, and S. Chowdhury, “Possible Causes & Solutions of Traffic Jam and Their Impact on the Economy of Dhaka City” *Journal of Management and Sustainability*, Volume 2, 2012.
- [14] K. He, X. Zhang, S. Ren, and J. Sun, “Deep residual learning for image recognition”, *arXiv preprint arXiv:1512.03385*, 2015.
- [15] R. Shamsher, and M. Abdullah, “Traffic Congestion in Bangladesh- Causes and Solutions: A study of Chittagong Metropolitan City,” *Asian Business Review*, Volume 2, March 2015.
- [16] A. Krizhevsky, I. Sutskever, and G. E. Hinton, “Imagenet classification with deep convolutional neural networks”, In *Advances in neural information processing systems*, pages 1097–1105, 2012
- [17] R. Girshick, J. Donahue, T. Darrell, and J. Malik, “Rich feature hierarchies for accurate object detection and semantic segmentation”, In *Proceedings of the IEEE Conference on Computer Vision and Pattern Recognition (CVPR)*, 2014.
- [18] N. Wang and D.-Y. Yeung, “Learning a deep compact image representation for visual tracking”, In *Advances in Neural Information Processing Systems*, pages 809–817, 2013.
- [19] J. Long, E. Shelhamer, and T. Darrell, “Fully convolutional networks for semantic segmentation”, In *Proceedings of the IEEE Conference on Computer Vision and Pattern Recognition*, pages 3431–3440, 2015.

- [20] A. Karpathy, G. Toderici, S. Shetty, T. Leung, R. Sukthankar, and L. Fei-Fei, "Large-scale video classification with convolutional neural networks", In *Computer Vision and Pattern Recognition (CVPR)*, 2014 IEEE Conference on, pages 1725–1732. IEEE, 2014.
- [21] A. Toshev and C. Szegedy, "DeepPose: Human pose estimation via deep neural networks", In *Computer Vision and Pattern Recognition (CVPR)*, 2014 IEEE Conference on, pages 1653–1660. IEEE, 2014.
- [22] C. Dong, C. C. Loy, K. He, and X. Tang, "Learning a deep convolutional network for image super-resolution", In *Computer Vision–ECCV 2014*, pages 184–199. Springer, 2014.
- [23] C. Szegedy, V. Vanhoucke, S. Ioffe, J. Shlens, and Z. Wojna, "Rethinking the inception architecture for computer vision", *arXiv preprint arXiv:1512.00567*, 2015.
- [22] J. Eriksson, L. Girod, B. Hull, R. Newton, S. Madden, and H. Balakrishnan, "The pothole patrol: using a mobile sensor network for road surface monitoring," In *Proceedings of the 6th international conference on Mobile systems, applications, and services (MobiSys'08)*, New York, USA, June 17 - 20, pp. 29-39.
- [23] M. Abadi, A. Agarwal, P. Barham, E. Brevdo, Z. Chen, C. Citro, G. S. Corrado, A. Davis, J. Dean, M. Devin, S. Ghemawat, I. Goodfellow, A. Harp, G. Irving, M. Isard, Y. Jia, R. Jozefowicz, L. Kaiser, M. Kudlur, J. Levenberg, D. Mane, R. Monga, S. Moore, D. Murray, C. Olah, M. Schuster, J. Shlens, B. Steiner, I. Sutskever, K. Talwar, P. Tucker, V. Vanhoucke, V. Vasudevan, F. Viegas, O. Vinyals, P. Wardén, M. Wattenberg, M. Wicke, Y. Yu, and X. Zheng. TensorFlow: Large-scale machine learning on heterogeneous systems, 2015. Software available from tensorflow.org.
- [24] A. Goswami and H. Liu, "Deep Dish: Deep Learning for Classifying Food Dishes," (2017) [Online], Available: <https://www.semanticscholar.org/paper/Deep-Dish-%3A-DeepLearning-for-Classifying-Food-Goswami/Microsoft/2e596abd9d4616f75c9da45d88787cb2fd5bee81>. [Accessed April 29, 2019].

- [25] J. H. Chuah, H. Y. Khaw, F. C. Soon and C. Chow, "Detection of Gaussian Noise and Its Level using Deep Convolutional Neural Network", Proc. of the 2017 IEEE Region 10 Conference (TENCON), Malaysia, November 5-8, 2017.
- [26] M. Teichmann, M. Weber, M. Zöllner, R. Cipolla and R. Urtasun, "MultiNet: Real-time Joint Semantic Reasoning for Autonomous Driving", IEEE Intelligent Vehicles Symposium, IV 2018, Changshu, China, June 26-30, 2018, pp. 1013-1020.
- [27] Y. Lyu, and X. Huang, "Road Segmentation Using CNN with GRU", 22nd International Conference on Information Visualization, 2018.
- [28] Z. Zhang, Q. Liu, Y. Wang. "Road extraction by deep residual U-net", IEEE Geosci. Remote Sens. Lett., vol. 15, no. 5, pp. 749-753, May 2018.
- [29] J. G. Haran, J. Dillenburg, and P. Nelson, "Realtime Image Processing Algorithms for the Detection of Road and Environmental Conditions", Ninth International Conference on Applications of Advanced Technology in Transportation, AATT 2006, Chicago, Illinois, August 13-15, 2006, pp. 55-60.
- [30] C. V. Dung and L. D. Anh, "Autonomous concrete crack detection using deep fully convolutional neural network", Automation in Construction, Volume 99, Pages 52-58, March 2019.
- [31] J. Zhao, H. Wu, and L. Chen, "Road Surface State Recognition Based on SVM Optimization and Image Segmentation Processing," Journal of Advanced Transportation, Vol 2017, pp. 1-21. 2017.
- [32] Z. Wan-zhi, W. Zeng-cai, "Rural Road Detection of Color Image in Complicated Environment", International Journal of Signal Processing, Image Processing and Pattern Recognition, Vol. 6, No. 6(2013), p.p. 161-168.
- [33] M. Lin, Q. Chen, and S. Yan, "Network in network", arXiv preprint arXiv:1312.4400, 2013.
- [34] K. Simonyan and A. Zisserman, "Very deep convolutional networks for large-scale image recognition", arXiv preprint arXiv:1409.1556, 2014.

- [35] C. Szegedy, W. Liu, Y. Jia, P. Sermanet, S. Reed, D. Anguelov, D. Erhan, V. Vanhoucke, and A. Rabinovich, "Going deeper with convolutions", In Proceedings of the IEEE Conference on Computer Vision and Pattern Recognition, pages 1–9, 2015.
- [36] J. Dean, G. Corrado, R. Monga, K. Chen, M. Devin, M. Mao, A. Senior, P. Tucker, K. Yang, Q. V. Le, et al. "Large scale distributed deep networks", In Advances in Neural Information Processing Systems, pages 1223–1231, 2012.
- [37] J. Eriksson, L. Girod, B. Hull, R. Newton, S. Madden, and H. Balakrishnan, "The pothole patrol: using a mobile sensor network for road surface monitoring," In Proceedings of the 6th international conference on Mobile systems, applications, and services (MobiSys'08), New York, USA, June 17 - 20, pp. 29-39.
- [38] H. Zhao, J. Shi, X. Qi, X. Wang, J. Jia, "Pyramid Scene Parsing Network", arXiv preprint arXiv:1612.01105v2[cs.CV] 27 Apr 2017.
- [39] V. Badrinarayanan, A. Kendall, & R. Cipolla (2017), Segnet: A deep convolutional encoder-decoder architecture for image segmentation, IEEE transactions on pattern analysis and machine intelligence, 39(12), 2481-2495.
- [40] M. Teichmann, M. Weber, M. Zoellner, R. Cipolla, & R. Urtasun, (2018, June), Multinet: Real-time joint semantic reasoning for autonomous driving. In 2018 IEEE Intelligent Vehicles Symposium (IV) (pp. 1013-1020). IEEE.
- [41] T. Pohlen, A. Hermans, M. Mathias, B. Leibe, "Full Resolution Residual Networks for Semantic Segmentation in Street Scenes", arXiv:1611.08323v2 [cs.CV] 6 Dec 2016.
- [42] Moran, Jeffrey, and Robert Desimone. "Selective attention gates visual processing in the extrastriate cortex." *Science* 229.4715 (1985): 782-784.
- [42] Fei-Fei Li, Justin Johnson and Serena Yeung. CS231n. Class Lecture, Topic: "Convolutional Neural Networks for Visual Recognition." Stanford University, Stanford, California 94305, Spring 2017.
- [43] Beck, Joseph E., and Beverly Park Woolf. "High-level student modeling with machine learning." *International Conference on Intelligent Tutoring Systems*. Springer, Berlin, Heidelberg, 2000.

- [44] Spanhol, Fabio Alexandre, et al. "Breast cancer histopathological image classification using convolutional neural networks." Neural Networks (IJCNN), 2016 International Joint Conference on. IEEE, 2016.
- [45] LeCun, Yann, Koray Kavukcuoglu, and Clément Farabet. "Convolutional networks and applications in vision." Circuits and Systems (ISCAS), Proceedings of 2010 IEEE International Symposium on. IEEE, 2010.
- [46] https://www.tensorflow.org/api_docs/python/tf/keras/initializers/HeUniform
- [47] Zou, Hui, and Trevor Hastie. "Regularization and variable selection via the elastic net." Journal of the Royal Statistical Society: Series B (Statistical Methodology) 67.2 (2005): 301-320.
- [48] Srivastava, Nitish, et al. "Dropout: A simple way to prevent neural networks from overfitting." The Journal of Machine Learning Research 15.1 (2014): 1929-1958.
- [49] Duchi, John, Elad Hazan, and Yoram Singer. "Adaptive subgradient methods for online learning and stochastic optimization." Journal of Machine Learning Research 12.Jul (2011): 2121-2159.
- [50] Zeiler, Matthew D. "ADADELTA: an adaptive learning rate method." arXiv preprint arXiv:1212.5701 (2012).
- [51] Hey, Anthony JG, and Anne E. Trefethen. "The data deluge: An e-science perspective." (2003): 809-824.
- [52] Hecht-Nielsen, Robert. "Theory of the backpropagation neural network." Neural networks for perception. 1992. 65-93.
- [53] Rumelhart, David E., Geoffrey E. Hinton, and Ronald J. Williams. "Learning representations by back-propagating errors." nature 323.6088 (1986): 533.
- [54] LeCun, Yann, et al. "Backpropagation applied to handwritten zip code recognition." Neural computation 1.4 (1989): 541-551.
- [55] Lei Zhang , Fan Yang , Yimin Daniel Zhang, and Y. J. Z., Zhang, L., Yang, F., Zhang, Y. D., & Zhu, Y. J. (2016). Road Crack Detection Using Deep Convolutional Neural Network.
- [56] https://gombru.github.io/2018/05/23/cross_entropy_loss/
- [57] <https://www.kaggle.com/docs/notebooks>
- [58] Chollet, François. "Keras." (2015): 128.

- [59] Goutte, Cyril, and Eric Gaussier. "A probabilistic interpretation of precision, recall and F-score, with implication for evaluation." European Conference on Information Retrieval. Springer, Berlin, Heidelberg, 2005.
- [60] S Maitra, RK Ojha and K Ghosh. 'Impact of Convolutional Neural Network Input Parameters on Classification Performance' 2018 4th International, 2018.
- [61] Diederik Kingma and Jimmy Ba from the University of Toronto in their 2015 ICLR paper (poster) title.

